The effects of some environmental factors on the photosynthesis of two brown algae, *Sargassum muticum* and *Sargassum macrocarpum* (Fucales) from Japan

（日本産褐藻タマハハキモクとノコギリモク（ヒバマタ目）の光合成における環境要因の影響）

ITO, Tomohiro

2022

The United Graduate School of Agricultural Sciences

Kagoshima University

This PhD. dissertation was based on the following articles published in the journals.

1. Ito T, Borlongan IA, Nishihara GN, Endo H, Terada R (2021) The effects of irradiance, temperature, and desiccation on the photosynthesis of a brown alga, *Sargassum muticum* (Fucales) from a native distributional range in Japan. J Appl Phycol 33: 1777–1791
2. Ito T, Yoshioka T, Shimabukuro H, Nishihara GN, Endo H, Terada R 2023. The effect of temperature, light-spectrum, desiccation, and salinity gradients on the photosynthetic performance of a subtidal brown alga, *Sargassum macrocarpum* from Japan. Phycol Res 71: (in press)

Abstract

The effects of some environmental factors including irradiance, light spectrum, temperature, desiccation, and salinity gradients on the photosynthesis of two brown algae, *Sargassum muticum* and *Sargassum macrocarpum* (Fucales) were determined using a pulse amplitude modulation (PAM)-chlorophyll fluorometer and optical dissolved oxygen sensors. In *S. muticum,* net photosynthesis–irradiance (*P–E*) curves at 8, 20, and 28°C showed that the net photosynthetic rate (NP_{max}) and saturation irradiance were highest at 28°C. Gross photosynthesis determined at 8–36°C and 300 µmol photons m^{-2} s^{-1} showed that the maximum gross-photosynthetic rate (GP_{max}) occurred at 19.5°C, which is consistent with the seawater temperature at its peaked abundance in Japan. The maximum quantum yield (F_v/F_m) during the 72-h temperature exposures were above 0.60 at 8–28°C but dropped at higher temperatures. Continuous exposure (12-h) to irradiance of 200 (low) and 1000 (high) µmol photons m^{-2} s^{-1} at three temperatures showed remarkable decline in the effective quantum yields ($\Delta F/F_m'$) under high irradiance at 8°C only; the F_v/F_m measured after 12-h dark acclimation also did not recover to initial values, signifying its sensitivity to photoinhibition at 8°C. In *S. macrocarpum*, *P–E* curves at 24°C under red (660 nm), green (525 nm), blue (450 nm), and white light (metal halide lamp) showed that NP_{max} under blue and white light was greater than under red and green

light, indicating the sensitivity and photosynthetic availability of blue light in the subtidal light environment. Temperature responses of the Fv/F_m (in darkness) and $\Delta F/F_m'$ (at 50 μmol photons m^{-2} s^{-1}) during 6-day culture (4–36°C) remained high at 12–28°C but decreased at higher temperatures. Nevertheless, $\Delta F/F_m'$ also dropped at temperatures below 8°C, suggesting light sensitivity under chilling temperatures, since F_v/F_m remained high. In the desiccation experiment, two species showed different responses under dehydrated and rehydrated states. In *S. muticum* that can be found in the lower intertidal and upper subtidal zones, this alga exhibited tolerance to 2-h of desiccation at 20°C and 50% humidity with 80% of water loss (absolute water content, AWC of 20%) from the thallus, and $\Delta F/F_m'$ recovered after 24-h of rehydration in seawater, suggesting potential of photosynthetic recovery of this alga at such low hydration threshold. In *S. macrocarpum* that can be found in the subtidal waters, this alga under aerial exposure of up to 8-h at 24°C and 50% humidity showed that $\Delta F/F_m'$ quickly declined after more than 45-min dehydration; furthermore, $\Delta F/F_m'$ also failed to recover to initial levels even after 1-day rehydration in seawater. Under the dehydrate state, the $\Delta F/F_m'$ remained high when the AWC was greater than 50%; in contrast, it quickly dropped when the AWC was less than 50%. When AWC is reduced below 50%, $\Delta F/F_m'$ did not return to initial levels, regardless of subsequent re-hydration, suggesting a low capacity of photosynthesis to

recover from desiccation. Furthermore, in the salinity response experiment conducted only for *S. macrocarpum*, it showed a stenohaline photosynthetic response between 20–40 psu, as their $\Delta F/F_m'$ were dropped at outside range of these salinities in 3-day culture. These results suggest that the reason why these two species are well adapted to each environment in the habitat and the range of distribution in Japan. Furthermore, the adaptation of *S. muticum* to relatively high irradiance, the broad range of temperature, and to desiccation may explain its potentially high invasive capacity.

1. Introduction

The communities of fucoid species, '*Gara-moba*' in Japanese, generally inhabit the lower intertidal and upper subtidal zones and are important primary producers within coastal ecosystems. These communities provide three-dimensional habitat for many associated biological organisms and are also a food source for herbivores (Murase *et al*. 2000a; Yatsuya *et al*. 2005; Longo *et al*. 2019; Wainwright *et al*. 2019; Terada *et al*. 2021a). The species of *Sargassum* (Sargassaceae, Fucales) can generally be found in all four major islands and the islands of the Ryukyu Archipelago of Japan (Yoshida 1983, 1998). In the temperate region of Japan that comprises of Honshu, Shikoku, and Kyushu Islands, more than thirty species of *Sargassum* including *Sargassum muticum* (Yendo) Fensholt and *Sargassum macrocarpum* C. Agardh compose the dense communities as the canopy-forming assemblages in upper subtidal and lower intertidal zones (Yoshida 1983, 1998, Terada *et al*. 2021a).

A species of *Sargassum*, *S. muticum* was originally described in 1907 from Kushimoto, Wakayama Prefecture, Honshu Island, Japan; it is endemic in the temperate coast of East Asia including Japan, Korea, and China (Yendo 1907; Yoshida 1983, 1998; Tseng and Lu 2000; Boo and Ko 2012). Nevertheless, this species is known as one of the most notorious invasive seaweeds in the world (Norton 1976; Rueness 1989; Stæhr *et al.*

2000). This alga was reported for the first time as an introduced species along the Pacific coast of North America in the first half of the 20th century (Scagel 1956; Abbott and Hollenberg 1976; Norton 1976; Norton and Benson 1983; Britton-Simmons 2004). It subsequently spread over 3000 km on the west coast of North America (Scagel 1956; Setzer and Link 1971; Britton-Simmons 2004). This species was also found in European waters at the Isle of Wight, England in 1973 (Farnham *et al.* 1973; Jones and Farnham 1973; Rueness 1989), and spread rapidly to other regions of Europe including the coasts of Great Britain, Ireland, and Iberian Peninsula, as well as throughout the North Sea, Baltic Sea, and Mediterranean Sea (e.g., Coppejans *et al*. 1980; Rueness 1989; Critchley 1983; Fernández 1999; Karlsson and Loo 1999; Engelen and Santos 2009; Critchley *et al.* 1990; Curiel *et al.* 1999).

The occurrence of invasive seaweeds may pose a threat to the native algal community by monopolizing space and competing with indigenous flora for resources (Williams and Smith 2007; Maggi *et al*. 2015). Indeed, the dominance of *S. muticum* in the non-native range has been a concern in the past few decades (Engelen *et al*. 2015); a number of studies related to the demography, phenology, and ecophysiology of the alga have been carried out to elucidate potential causes of its rapid expansion in the introduced areas and the impacts on the local ecosystem (e.g., Norton 1976; Deysher and Norton

1982; Espinoza 1990; Rico and Fernández 1997; Andrew and Viejo 1998; Stæhr *et al.* 2000; Wernberg *et al.* 2000; Hwang and Dring 2002; Steen and Rueness 2004). However, studies on this alga from the native range of distribution in East Asia remain insufficient especially in Japan, except for some growth and ecophysiological experiments (Uchida *et al.* 1991; Ogawa 1994; Liu *et al.* 2013; Xu *et al*. 2017). In Japan, *S. muticum* is found within the temperate coasts of Honshu, Shikoku, and Kyushu islands, which are particularly influenced by the warm *Kuroshio* and *Tsushima* currents (Yoshida 1983; Terada *et al*. 2020a, 2021a). This alga is rarely found in subarctic Hokkaido Island (except in the southern part of the island facing the Tsugaru Straits, i.e., Hakodate), as well as in the subtropical Ryukyu Islands and southern part of Kyushu Island (e.g., Kagoshima). *S. muticum* is known to be perennial and occurs on rocky substrata at the lower intertidal to upper subtidal zones during early spring through summer. Unlike other *Sargassum* species that form large and dense fucoid forests (e.g., *Sargassum patens* C. Agardh, *S. macrocarpum*; Murase *et al*., 2000a, b; Endo *et al*. 2019; Terada *et al*. 2018, 2020a, 2021a), this species is rather patchily distributed. Hence, introduced *S. muticum* may have distinct ecophysiological traits compared to individuals found in the species native range.

On the other hand, *S. macrocarpum* is the temperate species commonly found in Japan and Korea and is considered endemic only to these two countries (Yoshida 1983,

1998; Boo and Ko 2012; Cho *et al*. 2012; Titlyanov and Titlyanova 2012). Given that this alga forms dense and expansive populations on rocky substrata in the subtidal zone at depths ranging from 3–10 m, it can be regarded as one of the more deep-water-adapted fucoid species, especially when compared to other species of Japanese *Sargassum* (e.g., *Sargassum fusiforme* (Harvey) Setchell and *S. muticum*; Murase and Kito 2001; Murase *et al*. 2000a, b; Endo *et al*. 2013; Kokubu *et al*. 2015; Terada *et al*. 2020a). The daily relative compensation irradiance for *S. macrocarpum* was reported to be 1.3% of the light level at the sea surface, and the saturation irradiance for the instantaneous photosynthetic rates was also reported to be 105 μmol photons m^{-2} s^{-1} at 20°C, reinforcing the hypothesis that this species is adapted to deep-waters (Murase *et al*. 2000b; Terada *et al*. 2020a).

In recent years, we have great interest in revealing the ecophysiological responses of some *Sargassum* species under various environmental conditions, particularly irradiance and temperature gradients (Kokubu *et al*. 2015; Terada *et al*. 2016b, 2018, 2020a). For instance, the combined effects of low temperature and irradiance enhanced the photoinhibition of two temperate species, *S. patens* and *S. macrocarpum*, which provide a basis for understanding the persistence of these seaweeds at their respective higher latitudinal end of biogeographic ranges in the western Pacific (Terada *et al*. 2018, 2020a). However, the knowledge of this chilling-light sensitives has not been

elucidated for *S. muticum* as well as the temperature and irradiance response on the photosynthesis–temperature (*P*–*T*) and photosynthesis–irradiance (*P*–*E*) curves. As for *S. macrocarpum*, the threshold temperature under thermal stress (28°C) was reported based on the temperature response of the maximum quantum yield (F_v/F_m) of photosystem II (*PSII*) and oxygenic photosynthesis and dark respiration in relation to the natural distribution of this alga in Japan (Terada *et al*.2020a). This study suggested an upper limit on temperature with regards to photosynthesis; however, the lower limit of temperature remained to be revealed, given that the F_v/F_m (measured in darkness) was insensitive to cold temperature. In fact, the presence of light under low temperature was shown to induce a decline of the effective quantum yield ($\Delta F/F_m$) of *PSII* (e.g., *Caulerpa lentillifera* J. Agardh [Bryopsidales]; Terada *et al*. 2021c). With this perspective, explore the temperature response of photosynthesis with *S. macrocarpum* based on the $\Delta F/F_m$' measurement under the actual light environment is needed to be elucidated.

Like the knowledge of low-light adaptation in the subtidal environment, the knowledge of spectral light availability for the species of *Sargassum* is also essential for a better understanding of adaptation to the subtidal environment. In general, the visible spectrum of light ranges from about 380 to 750 nm, whereas photosynthetically active radiation ranges from 700 to 700 nm. Red light (625–780 nm) is important for

photosynthesis as it is mainly absorbed by chlorophyll *a*. However, red light is quickly reflected and absorbed near the sea surface and for subtidal species such as *S. macrocarpum*, red light can be deficient in their habitat. Nevertheless, light spectrum studies that focus on the photosynthesis of *S. macrocarpum* remain to be conducted.

In addition to temperature and irradiance responses, the ability to tolerate desiccation during tidal emersion influence the persistence of seaweeds in the intertidal to upper subtidal zones. The ability to withstand desiccation stress, characterized by fast recovery during rehydration, is the key factor determining their vertical distribution (Davison and Pearson 1996; Ji and Tanaka 2002). In our previous studies, desiccation and freezing tolerance was reported in a red alga, *Pyropia yezoensis* (Ueda) Hwang et Choi (= *Neopyropia yezoensis*; Bangiales), which enable populations of this species to flourish on the intertidal rocks during winter (Watanabe *et al*. 2017; Terada *et al*. 2020b). As *S. muticum* can be found in the lower intertidal and upper subtidal zones, this alga might have similar dehydration tolerance and a high-capacity recovery. In contrast, given that *S. macrocarpum* has never been found in the intertidal zone that is periodically exposed during low tides, its physiological tolerance to desiccation for this alga may be different from those of intertidal seaweeds including *S. muticum* that are influenced by extreme desiccation environments (Davison and Pearson 1996; Karsten 2012; Hurd *et al*. 2014).

Like desiccation, hypo- and hypersalinity environments are abiotic factors that cause osmotic stress in marine algae (Kirst 1990; Karsten 2012; Hurd *et al*. 2014). Especially, in the coastal environment in Japan, reduced salinity possibly occurs due to the freshwater from rivers and heavy rains that may constrain the occurrence and survival of marine algae from rocky intertidal regions and estuaries (Kirst 1990; Kameyama *et al*. 2021). In contrast, subtidal algae are generally believed to be sensitive to hypo- and hypersaline stress, as the salinity environment in the subtidal depth is almost stable (Norton and South 1969; Shindo *et al*. 2022). Probably, responses of photochemical efficiency in *S. macrocarpum* under desiccation and salinity gradients might be different from intertidal *S. muticum* and other algae in our past studies (Kameyama *et al*. 2021, Shindo *et al*. 2022).

In the present study, for two species of *Sargassum*, *S. muticum* and *S. macrocarpum* that can be found on the different habitats, we focused on to elucidating the effects of some environmental factors including temperature, irradiance, light spectrum, dehydration, and salinity gradients on the photosynthesis using the pulse amplitude modulation (PAM)-chlorophyll fluorometer and optical dissolved oxygen sensors. Specifically, for *S. muticum*, we examined the effect of irradiance and temperature on oxygenic photosynthesis (exp. 1 and 2), the single and combined effects of irradiance and temperature on the photochemical efficiency (exp. 3 and 4), and the

effect of desiccation on the photochemical efficiency (exp. 5). As for *S. macrocarpum*, we examined the effect of temperature on the photochemical efficiency (exp. 6), the effect of irradiance on oxygenic photosynthesis including the light spectral availability (exp. 7), and the effect of desiccation and salinity on the photochemical efficiency (exp. 8 and 9).

2. Materials and methods

2. 1. Sample collection and stock maintenance

Samples of *S. muticum* (more than 20 individuals for each experiment) were collected at a depth of 50 cm at low tide on 8 May 2017, 8 and 29 May 2018, and 7 May 2019 from Yura, Sumoto City, Awaji-shima Island, Hyogo Prefecture, Japan. Collected algae were transported to the laboratory of Kagoshima University in coolers at around 20°C, which was the seawater temperature during the sampling periods. Samples were maintained before examination in two aquarium tanks (200 L, respectively) at 33 psu, pH of 8.0–8.1, 20°C, and irradiance of ca. 40 μmol photons m^{-2} s^{-1} (14:10 hours light: dark cycle).

In contrast, those of *S. macrocarpum* were collected at Ihoda and Katashima, Yashiro-jima Island, Suo-Oshima Town, Yamaguchi Prefecture on 18 September 2020, and 29 March 2022. Additional samples were also collected on 16 October 2020 and 25 January 2021 to confirm the reproducibility of the irradiance experiment. Collected algae were transported to the laboratory in coolers at around 20°C, which was the seawater temperature during the sampling periods. Samples were maintained before examination in the aquarium tank (200 L) at 20–24°C, and irradiance of ca. 40 μmol photons m^{-2} s^{-1} (12:12 hours, 12L12D). The collected samples were continuously maintained in laboratory culture until the experiments were completed within a few weeks in every

sampling.

2. 2. The experiments for *S. muticum* study

2. 2. 1. Effect of irradiance on the oxygenic photosynthesis at 8, 20, and 28°C.

Net photosynthetic rates were determined at 0, 30, 60, 100, 150, 200, 250, 500, and 1000 mol photons m^{-2} s^{-1} (n = 5 per irradiance level), at 8, 20, and 28°C, respectively. These temperature treatments were based on the early-winter seawater temperature near the northern marginal region of distribution (January–February; Iwate Prefecture, Honshu Island; Yoshida *et al*. 1983; Terada *et al*. 2018, 2020), seawater temperature during its peaked abundance at the collection site (May–June; Terada *et al*. 2021), and the highest seawater temperature at the southern marginal region (August; Miyazaki Prefecture, Kyushu Island; Watanabe *et al*. 2014; Terada *et al*. 2018, 2020a), respectively.

Dissolved oxygen (DO) was measured using DO meters equipped with optical DO sensors (ProODO-BOD, YSI Incorporated, Yellow Springs, Ohio, USA). A metal-halide lamp was used as light source (MHN-150D-S, Nichido Ind. Co. Ltd, Osaka, Japan), and a spherical (4π) submersible quantum sensor (LI-193, LI-COR, Lincoln, Nebraska, USA) equipped light meter (LI-250A, LI-COR) was used to measure irradiance.

Methods for photosynthesis–irradiance (*P–E*) experiments were described in

detail in our previous studies (e.g., Terada *et al*. 2016 a, b, 2018, 2020a). Briefly, explants (i.e., fronds of the blade "leaf-like appendages" on the upper portion of algae; approximately 0.40 ± 0.01 g wet weight [8°C; g_{ww}; mean ± standard deviation, SD], 0.51 ± 0.01 g_{ww} [20°C], and 0.41 ± 0.02 g_{ww} [28°C]) were acclimated overnight (12 hours) with sterilized natural seawater in an incubator at each temperature treatment. On the day of the experiment, five explants were randomly selected and placed in 100 mL BOD bottles (YSI Japan's genuine product) containing sterilized natural seawater. The DO sensors were then inserted carefully into the BOD bottles so that no bubbles were trapped. DO concentrations (mg L^{-1}) were measured every 5 min for 30 minutes after a 30-min pre-acclimation to each experimental irradiance. Seawater was continuously stirred throughout the measurement, with the experimental temperatures maintained using a water bath with a circuit chiller (Coolnit CL-600R, Taitec, Inc., Tokyo, Japan). The exact volumes of the BOD bottles were determined after the experiment and were used to estimate photosynthesis and dark respiration rates. Seawater medium was renewed after each irradiance exposure and measurement to avoid any effects that can be attributed to nutrient and dissolved carbon dioxide depletion. The *P–E* experiments started at 0 μmol photons m^{-2} s^{-1} and finished at 1000 μmol photons m^{-2} s^{-1}. Dark respiration and net photosynthetic rates were estimated by fitting a first-order linear model to the collected

data.

2. 2. 2. Effect of temperature on the oxygenic photosynthesis and dark respiration

The measurements were conducted at eight temperatures (8, 12, 16, 20, 24, 28, 32, and 36°C; n = 5 per temperature) under an irradiance of 300 µmol photons m^{-2} s^{-1} (based on the saturation irradiance at 20°C). The different temperatures were obtained with a water bath. Similar to *P–E* experiments, explants (ca. 0.52 ± 0.03 g_{ww} SD) were derived from fronds of the blade (leaf-like appendages) on the upper portion of algae. DO concentrations were measured every 5 min over a 30-min interval, with 30 minutes of pre-acclimation to each temperature. Respiration rates were measured after 10 min of dark acclimation by wrapping the BOD bottles with aluminum foil.

2. 2. 3. Temperature effect on the photochemical efficiency of *PSII* over 72-hour exposure

The methods for this experiment were described in detail in our previous studies (e.g., Terada *et al*. 2018, 2020a). Mini Imaging-PAM (Heinz Walz GmbH, Effeltrich, Germany) measurements followed the procedure from our previous studies. At least 5 cm-long branches with the fronds of blades and vesicles from the upper portion of algae were cut

and acclimated overnight in the dark at 20°C. Sections (n = 10 per temperature) were haphazardly selected and placed in a stainless-steel tray (12×10×3 cm) containing sterilized natural seawater. Seawater temperature in the tray was controlled with an aluminum block incubator (BI-536T, Astec, Fukuoka, Japan), and monitored with a thermocouple (testo 925, testo AG, Lenzkirch, Germany). After a 10-minute dark acclimation phase, the maximum quantum yield of *PSII* (maximum photochemical efficiency of *PSII*, F_v/F_m [F_v/F_m = [F_m – F_o] / F_m]) at 0 µmol photons m^{-2} s^{-1} were measured to confirm the initial status (initial F_v/F_m). Sections were then placed in separate 500-mL flasks wrapped with aluminum foil and were incubated in the dark at nine temperatures (8, 12, 16, 20, 24, 28, 30, 32, and 36°C) for 72 hours (Eyela MTI-201B, Tokyo Rikakikai Co., LTD., Tokyo, Japan). F_v/F_m at each temperature was measured every 24 hours.

2. 2. 4. Combined effects of irradiance and temperature on the photochemical efficiency, and their potential of recovery

The methods for this experiment were described in detail in our previous studies (e.g., Terada *et al*. 2018, 2020a). The chronological change of effective quantum yields of *PSII* ($\Delta F/F_m'$ = *ΦPSII)* under a combination of irradiance (200 and 1000 µmol photons m^{-2} s^{-}

^{1}) and temperature (8, 20, and 28°C) was monitored during 12-hour exposure; their F_v/F_m were then measured after 12 hours of dark acclimation at each temperature. Initially, twenty branches (5 cm-long) with the fronds of blades and vesicles from the upper portion of algae were pre-incubated overnight (12 hours) in the dark at 8, 20, and 28°C, respectively. After pre-incubation, twenty explants from each temperature treatment were assigned to two PAR treatment groups (200 and 1000 µmol photons m^{-2} s^{-1}); their F_v/F_m (n = 10) at 0 µmol photons m^{-2} s^{-1} were measured to provide initial values. Samples were then placed in separate beakers (500 mL) containing sterile natural seawater maintained at a specific temperature in a water bath with a circuit chiller (Coolnit CL-150R, Taitec, Inc., Tokyo, Japan), and were exposed to either 200 or 1000 µmol photons m^{-2} s^{-1} (metal-halide lamp) for 12 hours. The explants were continuously stirred using magnetic stirrer to allow uniform light exposure on all replicates. The $\Delta F/F_m$' (n = 10 per temperature) were measured every one or two hours of continuous exposure to each irradiance treatment. Following the experiment, samples were once more dark-acclimated for 12 hours (almost the same period with the night-time in the natural state) at their respective temperatures; and their final F_v/F_m were measured to assess *PSII* recovery.

2. 2. 5. The effect of desiccation on the photochemical efficiency and the potential of

recovery after rehydration in seawater

To elucidate the status of $\Delta F/F_m'$ and the potential of recovery of desiccated thalli after subsequent rehydration in seawater, $\Delta F/F_m'$ (n = 50 per desiccation period) were determined at three different conditions i.e., after each desiccation period, 30 min and 24 h after rehydration in seawater. The methods for this experiment were followed from Terada *et al*. (2020b) with some modifications.

One day before the experiment, forty explants (branches with the fronds of blades and vesicles from the upper portion of algae) were pre-incubated overnight (12 hours) in the dark at 20°C for each irradiance experiment. After pre-incubation, five explants were assigned to eight desiccation treatments (0 [not desiccated], 0.5, 1, 2, 3, 4, 6, and 8-h air exposure period), respectively. To start the experiment, samples were then blot-dried in Kimwipes (Nippon Paper Crecia Co., Ltd, Tokyo, Japan), and placed on separate petri plates for the different desiccation treatments at 20°C, 20 µmol photons m^{-2} s^{-1}, and ca. 50% humidity. Thereafter, their $\Delta F/F_m'$ (n = 10 per explants; five explants at each desiccation period, i.e., total number of the measurements at each desiccation period is 50, n = 50 per period) at 20 µmol photons m^{-2} s^{-1} were measured at each desiccation period. The reason why ten different portions were measured from one individual was that the process of desiccation was not a uniform in the thallus (i.e., marginal and central

portions). A separate set of seaweed samples was used for the desiccation experiment at high irradiance (700 µmol photons m^{-2} s^{-1}) using white light-emitting diode (LED; CR-400L, Tomy Seiko Co., Ltd., Tokyo, Japan). We used the LED as light source for the desiccation experiment to avoid any thermal effect, as temperature was controlled in the cold room. Humidity was monitored during the experiment by a hygrometer (testo 610, testo AG, Lenzkirch, Germany).

The effect of chronic desiccation on water loss from the thallus was examined at dehydrated state, as well as after 30-min and 24-h rehydration. The absolute water content (AWC, %) after each desiccation period was calculated according to Eq. 1:

$$AWC\ (\%) = \frac{(W_t - W_d)}{(W_0 - W_d)} \times 100 \quad (1)$$

where W_t is the weight of the alga at time t after desiccation, W_0 is the initial weight of the alga (i.e., the wet weight after the gentle removal of surface moisture), and W_d is the dry weight of the alga after drying at 60°C in a sterilizer (MOV-202S, Sanyo Electric Co., Ltd., Osaka, Japan) for 48 h (Wang *et al*. 2011; Gao and Wang 2012; Gao *et al*. 2013; Watanabe *et al*. 2017). The weight of the samples was measured using an analytical balance (AB54-S, Mettler Toledo LLC, Columbus, Ohio, USA).

2. 3. The experiments for *S. macrocarpum* study

2. 3. 1. Photosynthesis–irradiance (*P–E*) curves under the different spectral light qualities

The experiments to determine the *P–E* curves were conducted under red, green, blue, and white light (Borlongan *et al*. 2020b). Each light spectrum was obtained using two-sets of LED arrays for red (646–664 nm [peak: 660 nm]; ISL-150X150-H4RR-SN, CCS Inc., Kyoto, Japan), green (510–543 nm [peak: 525 nm]; ISL-150X150-HGG), and blue light (444–467 nm [peak: 450 nm]; ISL-150X150-BB45), respectively. White light was obtained using a metal halide lamp (MHN-150D-S, Nichido Ind. Co. Ltd, Osaka, Japan).

The net photosynthetic rates were determined at 0 (dark respiration), 30, 60, 100, 150, 200, 250, 500, and 1000 μmol photons m^{-2} s^{-1} (n = 5 of the fronds of blade from different individuals) at 24°C. Irradiance was manipulated by adjusting the distance to the light source and confirmed using a spherical (4π) submersible quantum sensor equipped light meter. DO was monitored using DO meters equipped with optical dissolved oxygen sensors. Prior to each experiment, the fronds of blades at the lower and middle portions of algae (ca. 500 mg of wet weight for each replication) were cut and pre-incubated overnight with sterilized natural seawater in an incubator at 24°C (ca. 12 h).

The detailed measurement protocol was followed with those for *S. muticum* study and otherwise mentioned below. Irradiance was provided horizontally from one side of the aquarium by the metal halide lamp and LED, respectively. The experiments started at 0 μmol photons m^{-2} s^{-1} and finished at 1000 μmol photons m^{-2} s^{-1}. Dark respiration and net photosynthetic rates were estimated by fitting a first-order linear model to the collected data.

2. 3. 2. Temperature effect on the photochemical efficiency of *PSII* over 144-hour exposure

The fronds of the blades (ca. 1.5 cm long and wide) at the lower and middle portions of algae were acclimated overnight in the dark at 24°C (ca. 12 h). We assigned two irradiance levels (0 and 50 μmol photons m^{-2} s^{-1}) to assess the effects of temperature on the photochemical efficiency of *PSII* in darkness and under light-limited conditions (i.e., at levels below the saturation irradiance in the *P–E* curve). Samples (n = 10 per temperature) were then placed in the flasks (300mL) and were incubated at 10 temperature treatments (4, 8, 12, 16, 20, 24, 28, 30, 32, and 36°C) for 6 days in the dark (for the F_v/F_m measurement) and 50 μmol photons m^{-2} s^{-1} (for the $\Delta F/F_m'$ measurement; 12L12D photoperiod), respectively. The measurements of F_v/F_m (in darkness) and $\Delta F/F_m'$ (at 50

μmol photons m^{-2} s^{-1}) at each temperature level were conducted after 1, 3, and 6 days of culture. At every measurement, samples from the flasks were placed in sterilized natural seawater in a petri dish (9 cm diam.) on an aluminum block incubator. The detailed measurement protocol was followed those of the F_v/F_m measurement for *S. muticum* study.

2. 3. 3. The effect of desiccation on the photochemical efficiency and the potential of recovery after rehydration in seawater

The experimental design was followed those of *S. muticum* study with some modifications (Terada *et al*. 2021b, c). One day before the experiment, fronds of the blades (ca. 1.5 cm long and wide) at the lower and middle portions of algae were acclimated overnight in the dark at 24°C (ca. 12 hours). After pre-incubation, we assigned five explants to nine desiccation treatments (0 [not desiccated], 10-min, 30-min, 45-min, 1.0, 1.5, 2.0, 4.0, and 8.0-hour aerial exposure), respectively.

Initially, we selected the algal sections from the seawater medium, wiped the alga surface with Kimwipes, and placed them on separate Petri plates corresponding to each desiccation treatment at 24°C, 20 μmol photons m^{-2} s^{-1}, and ca. 50% humidity. At the end of each desiccation period, we recorded the $\Delta F/F_m'$ of *PSII* at 20 μmol photons m^{-2} s^{-1} using the Mini Imaging-PAM. Since the state of desiccation is not uniform in the

excised fronds (i.e., marginal and central portions), we measured ten different measuring portions per explant for five explants at each desiccation period; hence, there are five samples of which each sample consisting of 10 sub-samples across the excised frond. Humidity was monitored during the experiment by a hygrometer. After each desiccation period, we re-immersed the samples in seawater and measured the $\Delta F/F_m'$ of *PSII* at 30 min and 1 day after rehydration. The relationship between water loss from the frond and the $\Delta F/F_m'$ of *PSII* was also examined by measuring the initial wet-weight, wet-weight during the desiccated state, and final dry weight. The AWC (%) after each desiccation period was derived according to Eq. 1.

2. 3. 4. The effect of salinity on the photochemical efficiency of *PSII*

The effect of salinity on the photochemical efficiency of *PSII* was examined by measuring the $\Delta F/F_m'$ for 3 days. One day before the experiment, we cut the fronds of the blades (ca. 1.5 cm long and wide) at the lower and middle portions of algae and preincubated overnight in the dark at 24°C (ca. 12 hours). Before starting overnight preincubation, we measured the $\Delta F/F_m'$ of *PSII* under dim light (20 μmol photons m^{-2} s^{-1}) from 10 haphazardly selected segments using the Mini Imaging-PAM to identify the initial state (not shown in the result). The next day, we placed the samples (n = 10 per salinity

treatment) into the flasks (300 mL) of eleven salinity levels (0, 5, 10, 20, 30, 34, 40, 50, 60, 70, and 80 practical salinity unit, psu), and cultured for 3 days at 24°C under dim light (12L12D photoperiod). Note that 34 psu was the natural seawater salinity at the study site. Salinity was adjusted using distilled water and sodium chloride. However, dilution by freshwater causes the dilution of nutrients; therefore, we added Provasoli's enriched seawater with iodine (PESI) medium to all salinity levels following salinity adjustments to ensure no effect from the nutrients by levels. The measurements of $\Delta F/F_m'$ of PSII were conducted after 1-, 2-, and 3-days culture at 24°C under dim light.

2. 4. Modeling the photosynthetic response to temperature and irradiance

A Bayesian approach was used to analyze the response of photosynthesis to temperature. To model the response of either gross photosynthesis or maximum quantum yield to temperature, we applied a thermodynamic non-linear model (Eq. 2), which assumes that photosynthesis enters a less active state beyond some optimal temperature (Thornley and Johnson 2000; Alexandrov and Yamagata 2007). y is the response variable, which is either the gross photosynthetic rate or the maximum quantum yield (F_v/F_m). The temperature scale is Kelvin (K). The model has four parameters: y_{max} scales the model to the range of y. K_{opt} is the absolute temperature where y is maximized, H_a is the activation energy in kJ

mol^{-1} and H_d is the deactivation energy in kJ mol^{-1}. R in this model is the ideal gas constant, and has a value of 8.314 J K^{-1} mol^{-1}. The optimal value of y_{opt} at K_{opt} can be determined by substituting K_{opt} into the equation.

$$y = \frac{y_{max} \cdot H_d \cdot exp\left(\frac{H_a \cdot (K - K_{opt})}{K \cdot R \cdot K_{opt}}\right)}{\left(H_d - H_a \cdot \left(1 - exp\left(H_d \cdot \frac{(K - K_{opt})}{(K \cdot R \cdot K_{opt})}\right)\right)\right)} \quad (2)$$

The gross photosynthesis rate (*GP*), which is assumed as a hidden state, was estimated by simultaneously fitting the measured dark respiration rates (R_d) to the Arrhenius equation (Eq. 3), and the observed net photosynthesis rates to the difference in Eq. 2 and 3. Under light conditions, both photorespiration and non-photorespiratory (i.e., mitochondrial) reactions result in oxygen consumption (Tcherkez *et al*. 2008); however, it is not uncommon for the differences between respiration rates under light and dark conditions to be insignificant (Bellasio *et al*. 2014). Hence, photorespiration was assumed to be adequately described by the dark respiration rate. R_m is the respiration rate at the arbitrary reference temperature (i.e., mean temperature of 22°C; K_m = 295.15) and E_a is the activation energy.

$$R_d = R_m exp\left(-\frac{E_a}{R}\left(\frac{1}{K} - \frac{1}{K_m}\right)\right) \quad (3)$$

A zero inflated model (Eq. 4 and 5), in addition to Eq. 2, was applied to analyze F_v/F_m–temperature (F_v/F_m–T) responses, given the zero-valued observations that cannot be explained by Eq. 2 alone. The probability of zero (π) was estimated as a linear function of temperature on the logit scale.

$$f(y) = \pi + (1-\pi)g(0) \text{ if } y = 0 \quad (4)$$

$$f(y) = (1-\pi)g(0) \text{ if } y > 0 \quad (5)$$

The response of photosynthesis to irradiance was examined by modeling the data using an exponential equation (Jassby and Platt 1976; Webb *et al*. 1974; Platt *et al*. 1980; Henley 1993) which had the form:

$$NP_{net} = NP_{max}\left(1 - exp\left(\frac{-\alpha}{NP_{max}}E\right)\right) - R_d \quad (6)$$

where, NP_{net} is the net O_2 production rate, NP_{max} is the maximum O_2 production rate, α

is the initial slope of the *P–E* curve, *E* is the incident irradiance, and R_d is the dark respiration rate. From this model, the saturation irradiance (E_k) was calculated as NP_{max} / α and the compensation irradiance (E_c) was $NP_{max} ln\left(\frac{NP_{max}}{(NP_{max}-R_d)}\right)/\alpha$.

The response of $\Delta F/F_m'$ to AWC and salinity was examined by modeling the data using a generalized additive model (GAM) assuming a zero-inflated beta distribution for the error term (Eq. 7).

$$\begin{aligned} g(y) &= f(x) + f_i(x) + E_i \\ g(z) &= w(x) + w_i(x) + E_i \\ g(\delta) &= E_i \end{aligned} \qquad (7)$$

In Eq. 7, *x* is the predictor (i.e., AWC), *y* is the $\Delta F/F_m'$, *z* is the zero-inflation rate, and delta (δ) is the scale of the error distribution. *E* codes the experimental treatment as a factor, where *i* is the index for the experimental treatment. The functions *f* and *w* are thin-plate regression splines with the k-parameter set to 4. The function g is a logit function for *y* and *z* and a natural logarithm for delta. The null model estimated a global spline for *y* and *z*, and excluded the *E* term. A Student's t-distribution with 3 degrees-of-freedom, a location of zero, and a scale of 1was used for all model parameters.

2. 5. Statistical analyses

Statistical analyses were done using R version 4.1.3 (R Development Core Team 2022). *P–T* model fittings were done by directly using RStan version 2.19.3 (Stan Development Team 2020), while analyses for P–E and F_v/F_m–T responses were carried out through an interface provided by the R package brms version 2.16.3 (Bürkner 2018). The posterior distribution of the parameters was determined from four chains of run for 8000 samples per chain during the warmup phase and 2000 samples per chain thereafter. The chains were assessed visually and by examining the convergence statistic. The null model and the full model were compared using leave-one-out cross-validation (Bürkner 2018) and the model with the lowest leave-one out information criterion (looic) was determined to be the best fitting model.

A one-way ANOVA was used to examine if continuous irradiance exposures affected $\Delta F/F_m$' for each irradiance-temperature treatment. Time was considered a factor with levels: 0, 12, and 24 hours after the start of the experiment (i.e., initial F_v/F_m, $\Delta F/F_m$' after 12 h, and the final F_v/F_m after 12 hours of darkness). Differences in quantum yields of *S. muticum* in the desiccation-rehydration experiments over time at each irradiance were analyzed with one-factor ANOVA and with the fixed factor “desiccation period” (at

four levels: initial $\Delta F/F_m'$, $\Delta F/F_m'$ after desiccation period, and $\Delta F/F_m'$ after 30-min and 24-h rehydration in seawater).

3. Results

3. 1. The experiments for *S. muticum* study

3. 1. 1. Effect of irradiance on the oxygenic photosynthesis at 8, 20, and 28°C.

The oxygenic net photosynthetic (P_{net}) rates determined at 8, 20, and 28°C, steadily increased with increasing irradiance, and then approached saturation at the irradiance of more than 100 µmol photons m^{-2} s^{-1} (Fig. 1). At 8°C, P_{net} rates (mean ± standard deviation, SD) were -0.84 ± 0.12 µg O_2 g_{ww}^{-1} min^{-1} at 0 µmol photons m^{-2} s^{-1}, and 4.98 ± 0.73 µg O_2 g_{ww}^{-1} min^{-1} at 1000 µmol photons m^{-2} s^{-1} (Fig. 1a). Whereas at 20°C, P_{net} rates were -1.78 ± 0.05 µg O_2 g_{ww}^{-1} min^{-1} at 0 µmol photons m^{-2} s^{-1}, and 10.69 ± 1.61 µg O_2 g_{ww}^{-1} min^{-1} at 1000 µmol photons m^{-2} s^{-1} (Fig. 1b). Likewise, at 28°C, P_{net} rates were -4.13 ± 4.84 µg O_2 g_{ww}^{-1} min^{-1} at 0 µmol photons m^{-2} s^{-1}, and 19.80 ± 4.53 µg O_2 g_{ww}^{-1} min^{-1} at 1000 µmol photons m^{-2} s^{-1} (Fig. 1c).

Based on the *P–E* curves, the maximum net photosynthetic rates (NP_{max}) at 8, 20, and 28°C were estimated to be 5.16 (4.96–5.36 95% highest density credible interval, 95% HDCI), 11.88 (11.37–12.39 95% HDCI) and 28.12 (21.62–34.62 95% HDCI) µg O_2 g_{ww}^{-1} min^{-1}, respectively (Fig. 1, Table 1, Supplementary table 1). Likewise, saturation irradiance (E_k) increased with rise in temperature treatment and was 110 (98–121 95% HDCI), 200 (180–220 95% HDCI), and 753 (473–1034 95% HDCI) µmol photons m^{-2} s^{-}

^{1} at 8, 20, and 28°C, respectively. As shown in Table 1, the initial slopes (α) and dark respiration (R_d) rates were similar among the three temperatures. Hence, compensation irradiance (E_c) at these temperatures were comparable at 3 to 5 µmol photons m^{-2} s^{-1}.

3. 1. 2. Effect of temperature on the oxygenic photosynthesis and dark respiration

Measured *NP* rates at 300 µmol photons m^{-2} s^{-1} were variable across temperature gradients (8–36°C). Nevertheless, its response pattern appears to be represented by a dome-shaped curve (Fig. 2a). Dark respiration was likewise affected by temperature, with rates gradually increasing from 0.58 ± 0.28 (mean ± SD) µg O_2 g_{ww}^{-1} min^{-1} at 8°C to 5.72 ± 0.60 µg O_2 g_{ww}^{-1} min^{-1} at 36°C (Fig. 2c). The gross photosynthesis–temperature (*GP*–*T*) curve (Fig. 2b) derived from the P_{net}–temperature response and dark respiration indicated that the optimal temperature (T_{opt}^{GP}) at maximum gross photosynthetic rate (GP_{max} = 9.57 µg O_2 g_{ww}^{-1} min^{-1}) was 19.5°C (17.2–21.9 95% HDCI; Table 3). Model parameter estimates are presented in Table 2.

3. 1. 3. Effect of temperature on the photochemical efficiency of *PSII* over 72-hour exposure

The 72-hour temperature exposure experiment revealed that the F_v/F_m were almost stable

at values above 0.6 from 8 to 28°C (Fig. 3). In contrast, F_v/F_m at 32°C after 24 hours was 0.57 ± 0.02 (mean ± SD); it dropped to 0.29 ± 0.08 after 72 hours. Given the model and data after 24, 48, and 72-hour temperature exposures, maximum F_v/F_m ($F_v/F_{m(max)}$) at each exposure was 0.68 (0.67–0.68 95% HDCI), 0.68 (0.67–0.69 95% HDCI), and 0.67 (0.66–0.69 95% HDCI), respectively. Optimal temperature ($T_{opt}^{Fv/Fm}$) at each exposure period was 19.9°C (17.2–22.5°C 95% HDCI), 19.6°C (17.0–22.0°C 95% HDCI), and 23.5°C (22.1–24.8°C 95% HDCI), respectively. Other model parameter estimates are presented in Table 3.

3. 1. 4. Combined effects of irradiance and temperature on the photochemical efficiency, and their potential of recovery

Responses of the $\Delta F/F_m'$ during 12 hours of continuous exposures to 200 (low) and 1000 (high) μmol photons m^{-2} s^{-1} at 8, 20, and 28°C, and recovery of their F_v/F_m after 12 hours of dark acclimation were different among the irradiance-temperature treatments (Fig. 4).

At 8°C, the $\Delta F/F_m'$ of the alga throughout the 12-hour exposure to low irradiance maintained at 0.57 ± 0.03 (mean ± SD); such value was slightly lower than the initial F_v/F_m of 0.63 ± 0.02 ($P < 0.001$). Subsequent dark acclimation F_v/F_m returned to the initial level (0.62 ± 0.01, $P = 0.920$; Fig. 4a). In contrast, quantum yield of samples exposed to

high irradiance dropped from 0.65 ± 0.02 to 0.32 ± 0.06 (i.e., equivalent to 50.8% decrease in initial value, $P < 0.001$); its post-dark acclimation F_v/F_m (0.46 ± 0.06) was still significantly lower than its initial value ($P < 0.001$; Fig. 4b).

At 20°C, the $\Delta F/F_m'$ of alga exposed to low irradiance were stable throughout the irradiance exposure and dark acclimation periods (0.65 ± 0.02 initial F_v/F_m, 0.67 ± 0.03 $\Delta F/F_m'$ at 12-h exposure, and 0.61 ± 0.03 post-dark acclimation F_v/F_m; Fig. 4c). On one hand, the hourly response of the $\Delta F/F_m'$ in samples exposed to high irradiance slightly decreased; $\Delta F/F_m'$ after the 12-h exposure was 0.53 ± 0.03 ($P < 0.001$). Post-dark acclimation F_v/F_m of samples under high irradiance increased to 0.58 ± 0.02, but was still significantly lower than the initial F_v/F_m ($P < 0.001$; Fig. 4d).

At 28°C, the $\Delta F/F_m'$ of the alga exposed to low irradiance were likewise stable throughout the irradiance exposure and dark acclimation periods (0.62 ± 0.00 initial F_v/F_m; 0.62 ± 0.04 $\Delta F/F_m'$ at 12-h exposure, and 0.67 ± 0.04 post-dark acclimation F_v/F_m; Fig. 4e). The quantum yield of samples exposed to high irradiance declined from an initial F_v/F_m of 0.62 ± 0.02 to $\Delta F/F_m'$ of 0.55 ± 0.06 (= 11.3% decrease in initial value, $P < 0.001$). Final F_v/F_m after dark acclimation did not return to initial (0.55 ± 0.03, $P < 0.001$; Fig. 4f).

3. 1. 5. The effect of desiccation on the photochemical efficiency and the potential of recovery after rehydration in seawater

Under 20 μmol photons m^{-2} s^{-1}, $\Delta F/F_m'$ of the alga under aerial exposure remained stable from its initial value (0.67 ± 0.01; mean ± SD) until 0.5-h exposure (0.68 ± 0.04, P = 0.281; Fig. 5a). On one hand, $\Delta F/F_m'$ decreased with increasing desiccation period at 1-, 2-, and 3-h exposures (0.57 ± 0.17, P < 0.001 at 1-h; 0.53 ± 0.18, P < 0.001 at 2-h; and 0.26 ± 0.25, P < 0.001 at 3-h), and dropped to almost zero and zero at 4-, 6-, and 8-h exposures, respectively (0.04 ± 0.09, P < 0.001 at 4-h; 0.00 ± 0.02, P < 0.001 at 6-h; 0.00 ± 0.00 at 8-h).

The $\Delta F/F_m'$ of alga at desiccation treatments of 0.5-h exposure was also stable after samples were subjected to subsequent 30-min and 24-h rehydration in seawater (0.67 ± 0.01, P = 0.832 after 30-min rehydration; 0.69 ± 0.01, P < 0.001 after 24-h rehydration). Those at 1-h and 2-h desiccation treatments returned to the initial levels after 24-h rehydration in SW (0.69 ± 0.01, P < 0.001 at 1-h; 0.69 ± 0.01, P < 0.001 at 2-h). However, those at 3-, 4-, and 6-h air exposure failed to recover even after 24-h rehydration in seawater (0.58 ± 0.24, P < 0.001 at 3-h; 0.28 ± 0.33, P < 0.001 at 4-h; 0.06 ± 0.19, P < 0.001 at 6-h).

Under 700 μmol photons m^{-2} s^{-1}, $\Delta F/F_m'$ of the alga under aerial exposure quickly

declined from the initial value (0.67 ± 0.01; mean ± SD) until 2-h exposure (0.33 ± 0.12, $P < 0.001$ at 0.5-h exposure; 0.27 ± 0.19, $P < 0.001$ at 1-h; 0.03 ± 0.07, $P < 0.001$ at 2-h; Fig. 5b). $\Delta F/F_m'$ of the alga dropped to almost zero or zero after 8-h of aerial exposure. Following subsequent 30-min and 24-h rehydration in seawater, the $\Delta F/F_m'$ of alga returned to the initial level at the desiccation treatments of 0.5-h (0.66 ± 0.02, $P < 0.001$ after 30-min rehydration; 0.69 ± 0.01, $P < 0.001$ 24-h rehydration) and 1-h exposures (0.65 ± 0.02, $P < 0.001$ after 30-min rehydration; 0.68 ± 0.02, $P < 0.001$ after 24-h rehydration in SW). Those at 2-h desiccation treatments almost returned to the initial level after 24-h rehydration (0.65 ± 0.14, $P < 0.001$). However, those at 3-, 4-, and 6-h exposure failed to recover even after 24-h rehydration in seawater (0.00 ± 0.00, $P < 0.001$ at 3-h; 0.14 ± 0.27, $P < 0.001$, at 4-h; 0.00 ± 0.00, $P < 0.001$ at 6-h).

The fluctuation of the $\Delta F/F_m'$ of the alga was closely related to the decreasing absolute water content (AWC) of the thallus under desiccation (Fig. 6). Under the desiccation state at 20 μmol photons m^{-2} s^{-1} (Fig. 6a), the $\Delta F/F_m'$ was somewhat stable between 0.69 ± 0.01 and 0.61 ± 0.10 (mean ± SD, $n = 10$) during the AWC of 93.8% through 74.6%. However, it gradually decreased with decreasing AWC of below 72.0%, and dropped to zero at less than 20% AWC.

Likewise, those under the aerial desiccation state at 700 μmol photons m^{-2} s^{-1}

(Fig. 6b), declined with decreasing AWC, and dropped to zero at AWC of less than 20%. However, we did not obtain data for AWC between 60 and 99% due to the quick desiccation at relatively high irradiance. Nevertheless, those after 30-min and 24-h rehydration in seawater treatments at both 20 and 700 μmol photons m^{-2} s^{-1} (Fig. 6c, d, e, f), the $\Delta F/F_m'$ almost recovered to the initial level at AWC of above 20% (e.g., 0.69 ± 0.01 at AWC of 23.8%); however, those with less than 20% AWC did not recover even after 24-h rehydration in seawater.

3. 2. The experiments for *S. macrocarpum* study

3. 2. 1. Photosynthesis–irradiance (*P–E*) curves under the different spectral light qualities

The *P–E* curve of the net photosynthetic rates (P_{net}) was determined at 20°C under red, green, blue, and white lights (Fig. 7). Under white light, P_{net} rates were -2.71 ± 0.36 (mean ± SD) μg O_2 g_{ww}^{-1} min^{-1} at 0 μmol photons m^{-2} s^{-1}, 11.34 ± 2.65 (mean ± SD) μg O_2 g_{ww}^{-1} min^{-1} at 200 μmol photons m^{-2} s^{-1}, and 21.40 ± 2.26 (mean ± SD) μg O_2 g_{ww}^{-1} min^{-1} at 1000 μmol photons m^{-2} s^{-1} (Fig. 7A). Under red light, P_{net} rates were -1.51 ± 0.34 (mean ± SD) μg O_2 g_{ww}^{-1} min^{-1} at 0 μmol photons m^{-2} s^{-1}, 5.29 ± 1.18 (mean ± SD) μg O_2 g_{ww}^{-1} min^{-1} at 200 μmol photons m^{-2} s^{-1}, and 5.77 ± 2.35 μg O_2 g_{ww}^{-1} min^{-1} at 1000 μmol photons

m^{-2} s^{-1} (Fig. 7B). Under green light, P_{net} rates were -2.12 ± 0.24 µg O_2 g_{ww}^{-1} min^{-1} at 0 µmol photons m^{-2} s^{-1}, 6.47 ± 1.02 µg O_2 g_{ww}^{-1} min^{-1} at 200 µmol photons m^{-2} s^{-1}, and 11.07 ± 0.91 µg O_2 g_{ww}^{-1} min^{-1} at 1000 µmol photons m^{-2} s^{-1} (Fig. 7C). Under blue light, P_{net} rates were -2.38 ± 0.98 µg O_2 g_{ww}^{-1} min^{-1} at 0 µmol photons m^{-2} s^{-1}, 5.70 ± 3.33 µg O_2 g_{ww}^{-1} min^{-1} at 200 µmol photons m^{-2} s^{-1}, and 17.88 ± 3.32 µg O_2 g_{ww}^{-1} min^{-1} at 1000 µmol photons m^{-2} s^{-1} (Fig. 7D).

Based on the fitted photosynthesis – irradiance (*P–E*) curve, the maximum net photosynthetic rates (NP_{max}) under white, red, green, and blue lights were estimated to be 24.4 (22.6 – 26.0 95 % HDCI), 8.18 (6.68 – 9.73), 12.3 (10.6 – 14.0) and 22.1 (19.7 – 24.9) µg O_2 g_{ww}^{-1} min^{-1}, respectively (Fig. 7, Table 4). Compensation (E_c) and saturation irradiances (E_k) were also estimated to be 27.7 (18.9 – 35.9 95% HDCI) and 221 (187 – 261) µmol photons m^{-2} s^{-1} under white light, 19.9 (7.37 – 30.1) and 80.2 (48.7 – 123) µmol photons m^{-2} s^{-1} under red light, 23.5 (5.99 – 38.0) and 209 (140 – 308) µmol photons m^{-2} s^{-1} under green light, 52.2 (37.4 – 65.4) and 394 (305 – 514) µmol photons m^{-2} s^{-1} under blue light, respectively. The dark respiration (R_d) rate was similar among the light treatments and is shown in Table 4.

3. 2. 2. Effect of temperature on the photochemical efficiency of *PSII* over 144-hour

exposure

The response of F_v/F_m (at 0 μmol photons m^{-2} s^{-1}) after a 6-day exposure to a temperature range of 4 to 36°C was generally stable and temperature-independent with values above 0.500 from 8 to 28°C (Fig. 8A, B, C). The F_v/F_m at 30 and 32°C after 1-d exposure were 0.534 ± 0.024 and 0.395 ± 0.195 (mean ± SD), respectively; measured values dropped to 0.316 ± 0.018 and 0.000 ± 0.000 after three days, and to zero after six days. Given the model and data after 1-, 3-, and 6-d exposure, the maximum F_v/F_m ($F_v/F_{m(\max)}$: 0.651 [0.626 – 0.678, 95% highest density credible intervals, 95% HDCI] at 1-d, 0.632 [0.609 – 0.656] at 3-d, 0.603 [0.588 – 0.619] at 6-d) occurred at 21.8 (18.3 – 24.3 95% HDCI), 18.9 (13.6 – 22.7), and 20.1°C (14.9 – 27.0; $T_{opt}^{Fv/Fm}$), respectively (Table 5). Other model parameter estimates are presented in Table 5.

In contrast, the $\Delta F/F_m'$ (at 50 μmol photons m^{-2} s^{-1}) at 4 and 8°C after 1-d exposure were 0.192 ± 0.061(SD) and 0.269 ± 0.056, respectively (Fig. 8 D, E, F). This decline was consistent with those at 3- and 6-d exposure (0.226 ± 0.050 and 0.288 ± 0.073 after 3-d exposure, and 0.155 ± 0.042 and 0.270 ± 0.083 after 6-d exposure), respectively. Likewise, the $\Delta F/F_m'$ also dropped to almost zero at 32°C in 1-, 3-, and 6-d exposure (0.463 ± 0.057; 0.093 ± 0.187; 0.047 ± 0.140). Those at 36°C in 6-d exposure was fully dropped to zero. Given the model and data after 1-, 3-, and 6-d exposure, the maximum

$\Delta F/F_m'$ ($\Delta F/F_{m'(max)}$; 0.545 [0.526 – 0.567 95% HDCI] in 1-d; 0.634 [0.600 – 0.699] in 3-d; 0.582 [0.556 – 0.611] in 6-d) occurred at 20.5 (19.2 – 21.9 95% HDCI), 26.4 (25.1 – 27.7), and 22.4 °C (20.3 – 25.3; $T_{opt}^{\Delta F/Fm'}$), respectively (Table 6). Other model parameter estimates are presented in Table 6.

3. 2. 3. The effect of desiccation on the photochemical efficiency and the potential of recovery after rehydration in seawater

Under a desiccated state, the $\Delta F/F_m'$ of *PSII* was similar to initial values after 10- (0.613 ± 0.031 mean ± SD) and 30-min exposures (0.557 ± 0.053), but quickly decreased from the initial value (0.597 ± 0.027) and through 45- (0.494 ± 0.118), 60- (0.339 ± 0.197), 90- (0.121 ± 0.185), and 120-min exposure (0.1610± 0.185), dropping to almost zero (0.004 ± 0.014 after 240-min exposure) or zero (after 480-min exposure) at 240-min and beyond (Fig. 9A).

Under 30-min and 1-day rehydration (i.e., subsequent immersion) in seawater after each subsequent desiccation treatment, the $\Delta F/F_m'$ at desiccation treatments of 10-, and 30-min exposures remained near initial levels (0-min) after both subsequent 30-min (0.605 ±0.038 after 10-min exposure; 0.576 ± 0.039 after 30-min exposure) and 1-day (0.580 ± 0.066 after 10-min exposure; 0.583 ± 0.054 after 30-min exposure) rehydration in seawater. In contrast, the $\Delta F/F_m'$ that was dropped at 45-min exposure and more

prolonged exposures failed to recover regardless of 30-min (0.474 ± 0.458 after 45-min exposure; 0.294 ± 0.205 after 60-min exposure; 0.120 ± 0.176 after 90-min exposure; 0.145 ± 0.202 after 120-min exposure; 0.000 ± 0.000 after 240- and 480-min exposures) and 1-d rehydration (0.441 ± 0.202 after 45-min exposure; 0.253 ± 0.266 after 60-min exposure; 0.124 ± 0.212 after 90-min exposure; 0.162 ± 0.253 after 120-min exposure; 0.020 ± 0.049 after 240-min exposure; 0.017 ± 0.033 after 480-min exposure) in seawater.

The relationship between the $\Delta F/F_m'$ of *PSII* and water loss from the frond is shown in Fig. 10. The $\Delta F/F_m'$ when exposed in air ranged between 0.525 ± 0.074 (mean ± SD; 45-min exposure) and 0.641 ± 0.011(10-min exposure) and was relatively independent of the absolute water content (AWC) which ranged from 51.2% through 89.2% (Fig. 10A). However, the $\Delta F/F_m'$ gradually decreased as AWC decreased below 50% and dropped to zero as AWC decreased beyond 10%. Once the AWC declined below 50% under a desiccated state, the $\Delta F/F_m'$ did not recover even after 30-min (e.g., 0.306 ± 0.189 at AWC of 39.6%) and 1-day rehydration (0.257 ± 0.257 at AWC of 39.6%) in seawater (Fig. 10B, C).

The GAM fitted to this data indicated little influence of the experimental treatment on the expected value of $\Delta F/F_m'$ (Fig. 10). The expected value of $\Delta F/F_m'$ was generally stable for AWC greater than 50% and declined as AWC declined. The mean and

standard error of the looic of the null model was -278.8 ± 24.6and was lower than the full model (-268.6 ± 22.7), which suggests that experimental treatment (i.e., rehydration) had little to no effect on $\Delta F/F_m'$ recovery.

3. 2. 4. The effect of salinity on the photochemical efficiency of *PSII*

The $\Delta F/F_m'$ of *PSII* up to 3-day exposure under salinity gradient (0, 5, 10, 20, 30, 34, 40, 50, 60, 70, 80 psu) declined under hypo- and hypersaline stresses (Fig. 11; Table 7). Throughout the experiment, $\Delta F/F_m'$ remained stable between 20 (e.g., 0.554 ± 0.045 [mean ± SD] in 3-d) and 40 psu (0.595 ± 0.014 in 3-d), including the natural seawater salinity level (i.e. 34 psu; 0.602 ± 0014 in 3-d); however, there $\Delta F/F_m'$ clearly declined when salinity was10 psu (0.341 ± 0.222 in 1-d; 0.109 ± 0.198 in 2-d; 0.037 ± 0.111 in 3-d), and the $\Delta F/F_m'$ dropped to zero or almost zero at 0 and 5 psu throughout the experiment (0.096 ± 0.067 in 1-d; otherwise zero; Table 7). In addition, $\Delta F/F_m'$ at 50, 60, 70,80 psu also quickly dropped to zero or almost zero throughout the experiment (Table 7).

4. DISCUSSION

In Japan, *S. muticum* generally occurs on the lower intertidal to upper subtidal rocks at around 0.5–1 m deep during the spring low tide; therefore, the upper portion of the fronds can be emersed during daytime low tidal cycles and are subjected to relatively strong

incident irradiance (Kokubu *et al*. 2015; Terada *et al*. 2018). In contrast, as *S. macrocarpum* can be found on rocky substrata in the subtidal zone at depths ranging from 3–10 m, this alga is always immersed in seawater even in the tidal fluctuation. Despite the defference of the habitat depth, the geographical distributions of two species are mostly overlapped as these algae can be found along the coasts of Kyushu, Shikoku, and Honshu Islands of Japan that are influenced by warm *Kuroshio* and *Tsushima* currents (Yoshida 1983, 1989; Terada *et al*. 2021a). In fact, the range of seasonal fluctuation in seawater temperature at the habitat of this alga is known to be 13–28°C at the southern distributional limit (e.g., middle of Kyushu Island) and 7–25°C at northern distributional limit (e.g., northern end of Honshu Island) in Japan, respectively (Terada *et al*. 2016a; 2018, 2020, 2021a). Likewise, those at the sample collection site are also known to range from 10–26°C for *S. muticum* (Awaji-shima Island, Hyogo Prefecture) and from 9.5–27.5°C for *S. macrocarpum* (Yashiro-jima Island, Yamaguchi Prefecture), respectively (Yoshida and Shimabukuro 2017; Terada *et al*.2021a).

In the present study, the saturation irradiance (E_k) and maximum net photosynthesis (NP_{max}) in the oxygenic *P–E* curves of *S. muticum* at three temperatures (8, 20, and 28°C) were temperature-dependent. Lowest values occurred at 8°C while the highest was at 28°C, signifying that the light requirement to saturate net photosynthesis

is relatively increased with rising temperature, and so is the productivity of this alga at high ambient temperature. As compared with the past and present studies, E_k of *S. muticum* at 20 and 28°C (200 and 753 µmol photons m^{-2} s^{-1}, respectively) were somehow similar to those of other temperate Japanese *Sargassum* species, *S. patens* (289 and 401 µmol photons m^{-2} s^{-1} photons at 20 and 28°C) and *S. fusiforme* (Harvey) Setchell (391 µmol photons m^{-2} s^{-1} photons at 20°C) that are also found on the lower intertidal to upper subtidal zone, revealing their shared light-response adaptation in shallow-water habitat (Kokubu *et al*. 2015; Terada *et al*. 2018). On the other hand, the *P–E* curve of *S. macrocarpum* elucidated under white light at 24°C (221 µmol photons m^{-2} s^{-1}) in the present study is supported by past work determined at 8, 20, and 28°C (93, 105, and 213 µmol photons m^{-2} s^{-1}; Terada *et al*. 2020a), and the relatively low values of saturation (E_k) irradiances were thought to be related to the adaptation to the subtidal light environment (Murase *et al*. 2000b; Terada *et al*. 2020a). Under these light-limited environments, it is relevant to note that *S. macrocarpum* observed at relatively deep depths is longer and exhibits a less bush-like morphology (Endo *et al*. 2013). Perhaps, depth-related morphological characteristics may be a mechanism to overcome self-shading since self-shading would reduce the effective amount of light available for photosynthesis.

Aside from the degree of irradiance, the available light spectrum varies with

depth, as influenced by light penetration into oceanic or coastal waters. For instance, blue and green light wavelengths can penetrate relatively deep waters as compared to red light (Lüning 1990; Kirk 2011; Hurd *et al*. 2014). Adaptation to low irradiance and the spectral availability to the prevailing light environment at depth appear to be important strategies for algae to flourish in the habitat. In the present study, the *P–E* curves of *S. macrocarpum* determined under red, green, and blue light showed that the maximum net photosynthesis (NP_{max}) was greatest under blue light, and was fairly comparable to those under white light, thereby providing compelling evidence in support of the primary influence of blue light in the photosynthesis of this brown alga, as compared to red and green light (Dring 1989). Furthermore, as the E_k was also greatest under blue light, the quantity of blue light required to compensate for dark respiration and saturate photosynthesis appears to be greater than the other colors of light examined in the present study. In brown algae, blue light is known to be mainly absorbed by chlorophyll *a* (Soret band), chlorophyll *c*, and fucoxanthin (Kirk 2011; Hurd *et al*. 2014). Therefore, the blue light availability for photosynthesis in *S. macrocarpum* might be effectively absorbed by these photopigments and was considered to be one of the advantages allowing this alga to flourish in the subtidal waters. It is also important to note that *P–E* response of this alga under green light can also photosynthesize even though it was slightly lower than those under blue

light. In fact, the growth of *Sargassum horneri* (Turner) C. Agardh and *S. patens* under blue and green lights were likewise reported to be almost identical with those of under white light (Matsui *et al*. 1994). Further studies are needed for this insight including the composition and ratio of pigments in *S. macrocarpum*, as well as their respective absorption spectra. In fact, the overall photosynthetic performance of macroalgae is regarded to be quite complicated as the various types of photopigments are responsible for the different photosynthetic efficiencies under various light spectra (Falkowski and Raven 2007; Beer *et al*. 2014).

In the temperature response of *S. muticum*, temperature also influenced the oxygenic photosynthesis, dark respiration and *PSII* photochemical efficiency. Its temperature response of oxygenic photosynthesis (*GP* rates) revealed a characteristic single peak at 19.5°C (T_{opt}^{GP}), which is close to that of *S. fusiforme* (at 22.9°C; Kokubu *et al*. 2015). Despite the overlap of geographical distribution, optimum temperature for photosynthesis of *S. muticum* was lower than those of *S. patens* and *S. macrocarpum* (26.9°C and 27.8°C; Terada *et al*. 2018, 2020a). The T_{opt}^{GP} of two tropical Vietnamese species, *Sargassum mcclurei* Setchell and *Sargassum oligocystum* Montagne were even higher (32.9°C and 30.7°C; Terada *et al*. 2016b) compared to the above-mentioned temperate species. Indeed, *S. muticum* has spread outside its native range to relatively

higher latitudes in Europe and North America, suggesting the ability of the alga to photosynthesize at low water temperatures. Meanwhile, dark respiration increased with rising temperatures that resulted to the negative *NP* rates at high temperature (i.e., at 36°C).

As for the F_v/F_m response of *S. muticum* up to 72 hours of different temperature exposures, values were stable and relatively high from 8 to 28°C ($T_{opt}^{Fv/Fm}$ in 23.5°C, 72 h), but suddenly declined above 30°C. Such response is in parallel to its oxygenic *P–T* curve wherein *GP* rates are already decreasing at 28°C and above. Hence, this temperature can be regarded to be approaching critical threshold for heat stress, which may occur especially in the southern distributional limit of this alga in Miyazaki (31°48' N, 131°29' E), southern part of Kyushu Island facing the Pacific Ocean (Source: Herbarium of the Kagoshima University Museum). The highest summertime seawater temperature in Miyazaki reaches 28°C in August (Japan Oceanographic Data Center 2020). However, the F_v/F_m of *S muticum* was insensitive at low temperatures as compared to $\Delta F/F_m'$ measurements for *S. macrocarpum* study. Unfortunately, we could not have an opportunity to compare the temperature response of the F_v/F_m and $\Delta F/F_m'$ for *S. mutcum* in the present study, further studies for *S. muticum* are needed to compare the differences of these responses as described below for *S. macrocarpum.*

In the response to temperature of *S. macrocarpum*. The model to the $\Delta F/F_m'$ under a temperature gradient (4–36°C) after 6 days of culture revealed that the maximum $\Delta F/F_m'$ ($\Delta F/F_{m'(max)}$) occurred at 22.4°C (20.3–25.3; $T_{opt}^{\Delta F/Fm'}$) and dropped when temperatures were below 12°C or above 32°C, and corresponds well observations of water temperature in *S. macrocarpum* habitats in Japan, which includes those near the study site. In general, thermal stress is expected to influence the structural arrangement of the thylakoid membrane or accumulation of hydrogen peroxide that inhibits *de novo* synthesis of D_1 protein in *PSII* (Allakhverdiev and Murata 2004; Allakhverdiev *et al*. 2008; Takahashi and Murata 2008; Roleda 2009). Although we did not have the resources to confirm these details, we infer that the decline of photochemical efficiency at high temperature is related to these mechanisms.

The fitted model of the F_v/F_m measured in darkness in the 6-day culture revealed that the maximum F_v/F_m ($F_v/F_{m\ (max)}$) occurred at 20.1°C (14.9–27.0; $T_{opt}^{Fv/Fm}$) and dropped at above 30°C. Nevertheless, the temperature response of F_v/F_m was somewhat different from the $\Delta F/F_m'$, especially at low temperatures, and the F_v/F_m remained high and homogeneous within a range of 4–30°C and did not drop at low temperatures. The relatively high stability in F_v/F_m at a wide range of temperatures including low temperatures is supported by the past and present studies including this alga and *S. patens*

(Terada *et al*. 2018, 2020a). Indeed, in some marine macroalgae, F_v/F_m measured in darkness (after well acclimated in the dark) is less sensitive to temperature even at the low temperatures, and the presence of light at low temperatures enhances the depression of photochemical efficiency (Fukumoto *et al*. 2018, 2019; Terada *et al*. 2021c).

As for *S. muticum*, chronic (i.e., 12-h) temperature and irradiance exposures revealed absence of characteristic decline of the $\Delta F/F_m'$ at three temperatures (8, 20, 28°C) under low irradiance (200 µmol photons m^{-2} s^{-1}). However, the responses of $\Delta F/F_m'$ were different under high irradiance with apparent decline in $\Delta F/F_m'$ at 8°C, suggesting the influence of chilling-light stress on the seaweed (Terada *et al*. 2018, 2020a). The F_v/F_m of samples exposed to high irradiance at 8°C also failed to recover after the 12-hour dark acclimation, despite the 43.8% rise in 12-h exposed $\Delta F/F_m'$. Low temperature stress may have altered the repair of *PSII* that prevented its full recovery from photoinhibition. While F_v/F_m–temperature experiments under the dark showed relatively stable and high F_v/F_m throughout the 72-hour exposure at 8°C, this result needs to be interpreted with caution, as the presence of light may cause the acceleration of photodamage to *PSII* at low temperature. Results of the chronic irradiance–temperature experiments in the present study provided substantial evidence of the negative effects of high solar radiation and low temperature on the photosynthetic performance of this species at its northern limit of

natural distribution in southern Hokkaido and Aomori Prefectures (northernmost prefecture in Honshu Island; Yoshida 1983), where the mean winter seawater temperature is between 6 and 8°C (2002–2015; JODC 2020). In this marginal region, strong incident irradiance in winter primarily limits relative abundance of *S. muticum*. The present study also revealed that *S. muticum* can tolerate high irradiance at 20 and 28°C, unlike *S. patens* and *S. macrocarpum* that exhibited chronic photoinhibition at these temperatures (Terada *et al*. 2018, 2020a). Nevertheless, strategies and mechanisms that support the high invasive potential of *S. muticum* would be an interesting topic for further studies.

Regarding low-temperature stress in the photosynthesis, the fixation of carbon dioxide is believed to inhibit at low temperatures with a resultant generation of reactive oxygen species (ROS); consequently, the *de novo* synthesis of the D_1 protein is in turn suppressed, further reducing the *PSII* repair and resulting in severe damage to *PSII* (Allakhverdiev and Murata 2004). Along with the decline of the photochemical efficiency under low-temperature stress, the oxygen-evolving complex, light absorption antennae, reaction centers, electron acceptor and donor sides of *PSII* were reported to be damaged to varying degrees (e.g., *Kappaphycus alvarezii* [Doty] Doty ex Silva; Li *et al*. 2016). In the past and present studies, the F_v/F_m measured in darkness was often used to reveal the temperature response of photochemical efficiency (e.g., Terada *et al*. 2018, 2020a);

however, since $\Delta F/F_m'$ measured under light is more sensitive to temperature at lower temperatures, it might be more suitable than F_v/F_m when exploring the effects of low temperature.

Most *S. muticum* populations inhabit lower intertidal to upper subtidal zones which experience periodical emersion and submersion. As revealed in the desiccation experiment, the $\Delta F/F_m'$ under dehydrated state decreased with increasing air exposure period at both dim-light and high irradiances. The presence of strong light (700 μmol photons m^{-2} s^{-1}) may also have accelerated the water loss from the thallus, given the decline in $\Delta F/F_m'$ and AWC at a short desiccation time. Values dropped to almost zero at more than 2-h (high irradiance) or 3-h (dim-light) air exposures, with the absence of recovery after subsequent rehydration in seawater. Indeed, critical water loss was observed in samples under these desiccation treatments, with less than 50% AWC under two light treatments, which lead to reductions in $\Delta F/F_m'$. Nevertheless, the $\Delta F/F_m'$ under rehydrated state of *S. muticum* fully restored to the initial levels when the AWC under the dehydrate state maintained above 20%., suggesting the high capacity to recover the photochemical efficiency under such a critical dehydrate state.

In contrast, under an environment of 50% humidity, $\Delta F/F_m'$ of *S. macrocarpum* quickly decreased after more than 45 minutes of aerial exposure and never recovered to

initial level even after a 1-day rehydration in seawater, clearly indicated a poor tolerance to desiccation. Although a humidified environment to test the effects of desiccation may be less than ideal, especially given the subtidal habitat of *S. macrocarpum*, a decrease in AWC blow 50% clearly diminished the ability of photosynthesis activity to recover. This poor capacity to recover photosynthetic activity after desiccation is likely to be a common trait among subtidal alga, given that subtidal algae, such as *C. lentillifera* and *Saccharina japonica* (Areschoug) Lane Mayes, Druehl et Saunders (Laminariales) also had a poor capacity to recover after desiccation (Terada *et al*. 2021c; Shindo *et al*. 2022).

Photosynthetic activity is known to be negatively correlated with loss of water content in the cell (Dring and Brown 1982; Ji and Tanaka 2002; Contreras-Porcia *et al*. 2011; Hurd *et al*. 2014). Cellular dehydration due to desiccation after frond emersion is leads to an increase in electrolyte concentration within the cytoplasm, and changes membrane structures, including the thylakoid membrane (Wiltens *et al*. 1978; Kim and Garbary 2007). These structural changes can cause a decline in the photosynthesis activity by interrupting the electron flow between *PSI* and *PSII* (Gao *et al*. 2011). Likewise, the poor photosynthetic performance in desiccated algae can be associated with multiple cellular changes and loss of volume that resulted in general dysfunction of photosynthesis and include loss of repair capacity (e.g., *C. lentillifera*; Flores-Molina *et al*. 2014).

Intertidal algae adapted to such an extreme environment and can flourish in habitats that experience periodic cycles of immersion and emersion due to the tidal cycle (e.g., *Pyropia*, *Gracilaria*, etc.; Davison and Pearson 1996; Holzinger and Karsten 2013; Beer *et al*. 2014; Terada *et al*. 2021b; Kameyama *et al*. 2021). For example, in a red alga, *Gracilaria vermiculophylla* (Ohmi) Papenfuss (= *Agarophyton vermiculophyllum*), the $\Delta F/F_m'$ of PSII under a desiccated state with AWC above 20% recovered to initial levels following 1-day rehydration in seawater, demonstrating the potential for photosynthetic recovery in this alga from relatively low AWC (Kameyama *et al*. 2021). In the present study, *S.muticum* recovers photosynthesis when AWC exceeds 20%, whereas *S.macrocarpum* does not recover photosynthesis unless AWC exceeds 50%, showing different results. Adaptation to desiccation is likely to vary at the species level and is most likely dependent on the probability of emersion for a particular species.

As for the response to the salinity gradient, the $\Delta F/F_m'$ of *S. macrocarpum* in this study appeared to be stable within a relatively narrow range of salinity (20–40 psu) as observed from the 3-day culture, revealing stenohaline characteristics. In contrast, as the intertidal and estuary algae are sometimes influenced by rainfall and freshwater runoff, some algae, *S. fusiforme*, *G. vermiculophylla*, and *Pyropia tanegashimensis* (Shinmura) Kikuchi et Fujiyoshi (= *Phycocalidia tanegashimensis* [Shinmura] Santiañez; Bangiales)

are known to have a relatively strong tolerance to salinity, especially at low salinities (Gao *et al*. 2016; Xie *et al*. 2016; Kameyama *et al*. 2021; Xu *et al*. 2021; Yonemori *et al*. 2023). In fact, the $\Delta F/F_m'$ of *S. fusiforme* cultured between 10 – 50 psu did not decrease until three days, and those of *G. vermiculophylla* remained high until seven days culture of between 10 – 60 psu (Kameyama *et al*. 2021; Yonemori *et al*. 2023).

Hypo- or hypersaline stresses are ionic stresses (i.e., osmotic stresses), and is similar to dehydration stress. Under these salinity stresses, algal cells increase ionic concentrations but also undergo a change in ion ratios due to selective uptake. Therefore, photosynthesis and respiration of marine algae can be inhibited under these stresses (Kirst 1989), which may affect the initial charge separations at the reaction centers of *PSI* and *PSII*. In addition, osmotic stress appears to increase the permeability of the thylakoids to ions (e.g., Na^+, CI^-, K^+), which subsequently inhibit *PSI* and *PSII* (Kirst 1989). In contrast, under optimal salinities, the absence of these stresses may have resulted in high photosynthetic efficiency. Given that the habitat of *S. macrocarpum* does not occur near estuarine areas where salinity can vary over a relatively large range, the results of this study was not unexpected. Consider that the salinity of the habitat where the alga was collected ranged from 33 to 34 psu, hence the stenohaline characteristics elucidated in this study.

In conclusion, the adaptation of *S. muticum* to relatively high irradiance, the broad range of temperature (8–28°C), and to desiccation seems to be important to flourish at the intertidal to upper subtidal environments in Japan; moreover, this potential ability might also be an effective invasive advantage as an alien species. Given that this alga has an asexual reproduction, this ability for the self-fertilization also facilitates colonization success in novel habitats (Baker 1955; Krueger-Hadfield *et al.* 2016), thus invasions of this alga worldwide. Rapid adaptation to the novel habitat during invasion might result in phenotypic evolution (Sotka *et al*. 2018); hence, ecophysiological studies of this species in the non-native range of distribution are necessary. In contrast, the characteristics of photosynthesis of *S. macrocarpum* revealed in the present study, are regarded to be the factors to confine this alga to subtidal habitats, with little chance of emersion. The net photosynthetic response in *S. macrocarpum* is stronger under blue (and white) light, as opposed to red light, with a higher capacity for photosynthesis, suggesting the adaptation to the subtidal light environment. Desiccation negatively affects photosynthetic activity in this alga and inhibits the recovery of photosynthesis, regardless of rehydration for up to one day. Likewise, this alga poorly responds to hypo- and hyper-saline stress. The temperature response of photosynthesis supported to the past study and suggested adapting to the temperature environment in the temperate region of Japan. These insights

in the present study might also be effective especially for considering the optimal/critical environment (light, temperature, salinity, sample treatments, etc.) for the conservation /elimination of the natural / invaded communities.

Furthermore, *S. macrocarpum* poorly responds to hypo- and hyper- saline stress.

Acknowledgements

The author expresses his gratitude to Prof. Ryuta Terada, United Graduate School of Agricultural Sciences (UGSAS), Kagoshima University, and Prof. Gregory N. Nishihara, Institute for East China Sea Research, Organization for Marine Science and Technology, Nagasaki University, for their continuous support and valuable suggestions in the present study. Cordial thanks are doe to Prof. Tomoko Yamamoto, Faculty of Fisheries, Kagoshima University, and Prof. Hiroyuki Motomura, Kagoshima University Museum, and Dr. Hikaru Endo, Faculty of Fisheries, Kagoshima University, for their constructive comments and support during my study and the PhD dissertation committee. Finally, I would like to thank all lab mates at the Laboratory of Marine Botany for their advice and support during the research.

References

Abbott IA, Hollenberg GJ (1976) Marine Algae of California. Stanford University Press, Stanford

Alexandrov GA, Yamagata Y (2007) A peaked function for modeling temperature dependence of plant productivity. Ecol Model 200: 189–192

Allakhverdiev SI, Kreslavski VD, Klimov VV, Los DA, Carpentier R, Mohanty P (2008)

Heat stress: an overview of molecular responses in photosynthesis. Photosynth Res 98: 541–550

Allakhverdiev SI, Murata N (2004) Environmental stress inhibits the synthesis de novo of proteins involved in the photodamage-repair cycle of photosystem II in *Synechocystis* sp. PCC 6803. Biochimica et Biophysica Acta 1657: 23–32

Andrew NL, Viejo RM (1998) Ecological limits to the invasion of *Sargassum muticum* in northern Spain. Aqua Bot 60: 251–263

Baker HG (1955) Self-compatibility and establishment after 'long-distance' dispersal. Evolution 9: 347–349

Beer S, Biörk M, Beardall J (2014) Photosynthesis in the marine environment. Wiley-Blackwell, Ames, Iowa

Bellasio C, Burgess SJ, Griffiths H, Hibberd JM (2014) A high throughput gas exchange screen for determining rates of photorespiration or regulation of C4 activity. J Exp Bot 65: 3769–3779

Boo SM, Ko YD (2012) Marine plants from Korea. Marine and Extreme Genome Research Centre Program, Seoul (in Korean)

Borlongan IA, Suzuki S, Nishihara GN, Kozono J, Terada R (2020b) Effects of light quality and temperature on the photosynthesis and pigment content of a subtidal

edible red alga *Meristotheca papulosa* (Solieriaceae, Gigartinales) from Japan. J Appl Phycol 32: 1329–1340

Britton-Simmons KH (2004) Direct and indirect effects of the introduced alga *Sargassum muticum* on benthic, subtidal communities of Washington State, USA. Mar Ecol Prog Ser 277: 61–78

Bürkner PC (2018) Advanced Bayesian Multilevel Modeling with the R Package brms. The R Journal 10: 395–411

Cho SM., Lee SM., Ko YD, Mattio L, Boo SM (2012) Molecular systematic reassessment of *Sargassum* (Fucales, Phaeophyceae) in Korea using four gene regions. Bot Mar 55: 473–484

Contreras-Porcia L, Thomas D, Flores V, Correa JA (2011) Tolerance to oxidative stress induced by desiccation in *Porphyra columbina* (Bangiales, Rhodophyta). J Exp Bot 62: 1815–1829

Coppejans E, Rappe G, Podoor N, Asperges M (1980) *Sargassum muticum* (Yendo) Fensholt ook langs de Belgische kust Aangespoeld. Dumortiera 16: 7–13

Critchley AT (1983) *Sargassum muticum*: a taxonomic history including world-wide and western pacific distributions. J Mar Biol Assoc UK 63: 617–625

Critchley AT, Farnham WF, Yoshida T, Norton TA (1990) A bibliography of the invasive

alga *Sargassum muticum* (Yendo) Fensholt (Fucales, Sargassaceae). Bot Mar 33: 551–562

Curiel D, Bellemo G, Marzocchi M, Scattolin M, Parisi G (1999) Distribution of introduced Japanese macroalgae *Undaria pinnatifida*, *Sargassum muticum* (Phaeophyta) and *Antithamnion pectinatum* (Rhodophyta) in the Lagoon of Venice. Hydrobiologia 385: 17–22

Davison IR, Peason GA (1996) Stress tolerance in intertidal seaweeds. J Phycol 32: 197–211

Deysher L, Norton TA (1982) Dispersal and colonization in *Sargassum muticum* (Yendo) Fensholt. J Exp Mar Biol Ecol 56:179–195

Dring MJ (1989) Stimulation of light-saturated photosynthesis in *Laminaria* (Phaeophyta) by blue light. J Phycol 25: 254–258

Dring MJ, Brown FA (1982) Photosynthesis of intertidal brown algae during and after periods of emersion: a renewed search for physiological causes of zonation. Mar Ecol Prog Ser 8: 301–308

Endo H, Nishigaki T, Yamamoto K Takeno K (2013) Age- and size-based morphological comparison between the brown alga *Sargassum macrocarpum* (Heterokonta; Fucales) from different depths at an exposed coast in northern Kyoto, Japan. J

Appl Phycol 25: 1815–1822

Endo H, Nishigaki T, Yamamoto K, Takeno K (2019) Subtidal macroalgal succession and competition between the annual, *Sargassum horneri*, and the perennials, *Sargassum patens* and *Sargassum piluliferum*, on an artificial reef in Wakasa Bay, Japan. Fish Sci 85: 61–69

Engelen A, Santos R (2009) Which demographic trails determine population growth in the invasive brown seaweed *Sargassum muticum*? J Ecol 97: 675–684

Engelen A, Serebryakova A, Ang P, Britton-Simmons K, Mineur F, Pedersen MF, Arenas F, Fernández C, Steen H, Svenson R, Pavia H, Toth G, Viard F, Santos R (2015) Circumglobal invasion by the brown seaweed *Sargassum muticum*. Oceanogr Mar Biol An Annu Rev 53: 81–126

Espinoza J (1990) The southern limit of *Sargassum muticum* (Yendo) Fensholt (Phaeophyta, Fucales) in the Mexican Pacific. Bot Mar 33: 193–196

Falkowski PG, Raven JA (2007) Aquatic photosynthesis. Second edition. Princeton University Press, Princeton and Oxford

Farnham WF, Fletcher RL, Irvine LM (1973) Attached *Sargassum muticum* found in Britain. Nature 243: 231–232

Fernández C (1999) Ecology of *Sargassum muticum* (Phaeophyta) on the north coast of

Spain: IV. Sequence of colonization on a shore. Bot Mar 42: 553–562

Fukumoto R, Borlongan IA, Nishihara GN, Endo H, Terada, R (2018) The photosynthetic responses to PAR and temperature including chilling-light stress on the heteromorphic life history stages of a brown alga, *Cladosiphon okamuranus* (Chordariaceae) from Ryukyu Islands, Japan Phycol Res 66: 209–217

Fukumoto R, Borlongan, IA, Nishihara GN, Endo H, Terada R (2019) Effect of photosynthetically active radiation and temperature on the photosynthesis of two heteromorphic life history stages of a temperate edible brown alga, *Cladosiphon umezakii* (Chordariaceae, Ectocarpales), from Japan. J Appl Phycol 31: 1259–1270

Gao S, Huan L, Lu XP, Jin WH, Wang XL, Wu ML, Wang GC (2016) Photosynthetic responses of the low intertidal macroalga *Sargassum fusiforme* (Sargassaceae) to saline stress. Photosynthetica 54: 430–437

Gao S, Niu J, Chen W, Wang G, Xie X, Pan G, Gu W, Zhu D (2013) The physiological links of the increased photosystem II activity in moderately desiccated *Porphyra haitanensis* (Bangiales, Rhodophyta) to the cyclic electron flow during desiccation and re-hydration. Photosyn Res 116: 45–54

Gao S, Shen S, Wang G, Niu J, Lin A, Pan G (2011) PSI-driven cyclic electron flow

allows intertidal macro-algae *Ulva* sp. (Chlorophyta) to survive in desiccated conditions. Plant Cell Physiol 52: 885–893

Gao S, Wang G (2012) The enhancement of cyclic electron flow around photosystem I improves the recovery of severely desiccated *Porphyra yezoensis* (Bangiales, Rhodophyta). J Exp Bot 63: 4349–4358

Henley WJ (1993) Measurement and interpretation of photosynthetic light-response curves in algae in the context of photo inhibition and diel changes. J Phycol 29: 729–739

Holzinger A, Karsten U (2013) Desiccation stress and tolerance in green algae: consequences for ultrastructure, physiological, and molecular mechanisms. Front Plant Sci 4: article 327

Hurd CL, Harrison PJ, Bischof K, Lobban CS (2014) Seaweed ecology and physiology, 2nd Edition. Cambridge University Press, Cambridge

Hwang EK, Dring MJ (2002) Quantitative photoperiodic control of erect thallus production in *Sargassum muticum*. Bot Mar 45:471–475

Japan Oceanographic Data Center (2020) Fixed Station Temperature Data. JODC Data On-line Service System. URL https://jdoss1.jodc.go.jp/vpage/coastal.html (accessed on 13 June 2020)

Jassby AD, Platt T (1976) Mathematical formulation of the relationship between photosynthesis and light for phytoplankton. Limnol Oceanogr 21: 540–547

Ji Y, Tanaka J (2002) Effect of desiccation on the photosynthesis of seaweeds from the intertidal zone in Honshu, Japan. Phycol Res 50: 145–153

Jones G, Farnham WF (1973) Japweed: new threat to British coasts. New Scientist 60: 394–395

Kameyama R, Nishihara GN, Kawagoe C, Terada R (2021) The effects of four stressors, irradiance, temperature, desiccation, and salinity on the photosynthesis of a red alga, *Agarophyton vermiculophyllu*m (Gracilariales) from a native distributional range in Japan. J Appl Phycol 33: 2561–2575

Karlsson J, Loo LO (1999) On the distribution and the continuous expansion of the Japanese seaweed *Sargassum muticum* in Sweden. Bot Mar 42: 285–294

Karsten U (2012) Seaweed acclimation to salinity and desiccation stress. In: Wiencke, C. and Bischof, K. (Eds) Seaweed biology. Novel insights into ecophysiology, ecology and utilization (Ecological studies book 219). Springer-Verlag Berlin Heidelberg, Berlin, pp. 87–107

Kim KY, Garbary DJ (2007) Photosynthesis in *Codium fragile* (Chlorophyta) from a Nova Scotia estuary: responses to desiccation and hyposalinity. Mar Biol 151: 99–

107

Kirk JT (2011) Light and photosynthesis in aquatic ecosystem, Third edition. Cambridge University Press, Cambridge

Kirst GO (1990) Salinity tolerance of eukaryotic marine algae. Annu Rev Plant Physiol Plant Mol Biol 41: 21–53

Kokubu S, Nishihara GN, Watanabe Y, Tsuchiya Y, Amano Y, Terada R (2015) The effect of irradiance and temperature on the photosynthesis of a native brown alga, *Sargassum fusiforme* (Fucales) from Kagoshima, Japan. Phycologia 54: 235–247

Krueger-Hadfield SA, Kollars NM, Byers JE, Greig TW, Hammann M, Murray DC, Murren CJ, Strand AE, Terada R, Weinberger F, Sotka EE (2016) Invasion of novel habitats uncouples haplo-diplontic life cycles. Molecular Ecology 25: 3801–3816

Li H, Liu J, Zhang L, Pang T (2016) Effects of low temperature stress on the antioxidant system and photosynthetic apparatus of *Kappaphycus alvarezii* (Rhodophyta, Solieriaceae). Mar Biol Res 12: 1064–1077

Liu F, Pang S, Gao S, Shan T (2013) Intraspecific genetic analysis, gamete release performance, and growth of *Sargassum muticum* (Fucales, Phaeophyta) from China. Chin J Oceanol Limnol 31: 1268–1275

Longo P, Mansur K, Leite F, Passos F (2019) The highly diverse gastropod assemblages associated with *Sargassum* spp. (Phaeophyceae: Fucales) habitats. J Mar Biol Assoc U K 99: 1295–1307

Lüning K (1990) Seaweeds. Their environment, biogeography, and ecophysiology. Wiley-Interscience, New York

Maggi E, Benedetti-Cecchi L, Castelli A, Chatzinikolaou E, Crowe TP, Ghedini G, Kotta J, Lyons DA, Ravaglioli C, Rilov G, Rindi L, Bulleri F (2015) Ecological impacts of invading seaweeds: a meta-analysis of their effects at different trophic levels. Diversity Distrib 21: 1–12

Matsui T, Ohgai M, Murase N (1994) The effects of light quality on germling and thallus growth in *Sargassum horneri* and *S. patens*. Nippon Suisan Gakkaishi 60: 727–733 (in Japanese with English summary)

Murase N, Kito H, Mizukami Y, Maegawa M (2000a) Productivity of *Sargassum macrocarpum* (Fucales, Phaeophyta) population in Fukawa Bay, Sea of Japan. Fish Sci 66: 270–277

Murase N, Kito H, Mizukami Y, Maegawa M (2000b) Relationship between critical photon irradiance for growth and daily compensation point of juvenile *Sargassum macrocarpum*. Fish Sci 66: 1032–1038

Norton TA (1976) Why is *Sargassum muticum* so invasive? British Phycol J 11: 197–198

Norton TA, Benson MR (1983) Ecological interactions between the brown seaweed *Sargassum muticum* and its associated fauna. Mar Biol 75: 169–177

Norton TA, South R (1969) Influence of reduced salinity on the distribution of two laminaran algae. Oikos 20: 320–326

Ogawa H (1994) Effects of temperature and salinity on the rhizoid development of *Sargassum muticum*. Suisanzoshoku 42: 25–31 (in Japanese with English abstract)

Platt T, Gallegos CL, Harrison WG (1980) Photoinhibition of photosynthesis in natural assemblages of marine phytoplankton. J Mar Res 38: 687–701

R Development Core Team (2020) R: A language and environment for statistical computing. R Foundation for Statistical Computing, Vienna, Austria. ISBN 3-900051-07-0, URL http://www.R-project.org (acessed on 10 June 2020)

Rico JM, Fernández C (1997) Ecology of *Sargassum muticum* on the North coast of Spain. II. Physiological differences between *Sargassum muticum* and *Cystoseira nodicaulis*. Bot Mar 40: 405–410

Roleda MY (2009) Photosynthetic response of Arctic kelp zoospores exposed to radiation and thermal stress. Photobiol Sci 8: 1302–1312

Rueness J (1989) *Sargassum muticum* and other introduced Japanese macroalgae:

biological pollution of European coasts. Mar Poll Bull 20: 173–176

Scagel RF (1956) Introduction of a Japanese alga, *Sargassum muticum* into the northeast Pacific. Fisheries Research Papers. Department of Fisheries, State of Washington 1: 49–59

Setzer B, Link C (1971) The wanderings of *Sargassum muticum* and other relations. Stomatopod 2: 5–6

Shindo A, Nishihara GN, Borlongan IA, Terada R (2022) The effects of desiccation and salinity gradients in the photochemical efficiency of a subtidal brown alga, *Saccharina japonica* (Laminariales) from Hokkaido, Japan. Phycol Res 70: 89–96

Sotka EE, Baumgardner AW, Bippus PM, Destombe C, Duermit EA, Endo H, Flanagan BA, Kamiya M, Lees LE, Murren CJ, Nakaoka M, Shainker SJ, Strand AE, Terada R, Valero M, Weinberger F, Krueger-Hadfield SA (2018) Combining niche shift and population genetic analyses predicts rapid phenotypic evolution during invasion. Evol Appl 11: 781–793

Stan Development Team (2020) Stan: A C++ Library for Probability and Sampling, Version 2.18.9. URL: http://mc-stan.org (acessed on 10 April 2020)

Steen H, Rueness J (2004) Comparison of survival and growth in germlings of six fucoid

species (Fucales, Phaeophyceae) at two different temperature and nutrient levels. Sarsia 89: 175–183

Stæhr PA, Pedersen MF, Thomsen MS, Wernberg T, Krause-Jensen D (2000) Invasion of *Sargassum muticum* in Limfjorden (Denmark) and its possible impact on the indigenous macroalgal community. Mar Ecol Prog Ser 207: 79–88

Takahashi S, Murata N (2008) How do environmental stresses accelerate photoinhibition? Trends Plant Sci **13**: 178–182

Tcherkez G, Bligny R, Gout E, Mahé A, Hodges M, Cornic G (2008) Respiratory metabolism of illuminated leaves depends on CO_2 and O_2 conditions. Proc Natl Acad Sci USA 105: 797–802

Terada R, Abe M, Abe T, Aoki M, Dazai A, Endo H, Kamiya M, Kawai H, Kurashima A, Motomura T, Murase N, Sakanishi Y, Shimabukuro H (2021a) Japan's nationwide long-term monitoring survey of seaweed communities known as the "*Monitoring Sites 1000*": Ten-year overview and future perspectives. Phycol Res 69: 12–30

Terada R, Matsumoto K, Borlongan IA, Watanabe Y, Nishihara GN, Endo H, Shimada S (2018) The combined effects of PAR and temperature including the chilling-light stress on the photosynthesis of a temperate brown alga, *Sargassum patens* (Fucales), based on field and laboratory measurements. J Appl Phycol 30: 1893–

1904

Terada R, Nakashima Y, Borlongan IA, Shimabukuro H, Kozono J, Endo H, Shimada S, Nishihara GN (2020a) Photosynthetic activity including the thermal- and chilling-light sensitivities of a temperate Japanese brown alga *Sargassum macrocarpum*. Phycol Res 68: 70–79

Terada R, Nishihara GN, Arimura K, Watanabe Y, Mine T, Morikawa T (2021b) Photosynthetic response of a cultivated red alga, *Neopyropia yezoensis* f. *narawaensis* (= *Pyropia yezoensis* f. *narawaensis*; Bangiales, Rhodophyta) to dehydration stress differs with between two heteromorphic life-history stages. Algal Res 55: 102262

Terada R, Shikada S, Watanabe Y, Nakazaki Y, Matsumoto K, Kozono J, Saino N, Nishihara GN (2016a) Effect of PAR and temperature on the photosynthesis of Japanese alga, *Ecklonia radicosa* (Laminariales), based on field and laboratory measurements. Phycologia 55: 178–186

Terada R, Takaesu M, Borlongan IA, Nishihara GN (2021c) The photosynthetic performance of a cultivated Japanese green alga *Caulerpa lentillifera* in response to three different stressors, temperature, irradiance, and desiccation. J Appl Phycol 33: 2547–2559

Terada R, Vo TD, Nishihara GN, Matsumoto K, Kokubu S, Watanabe Y, Kawaguchi S (2016b) The effect of PAR and temperature on the photosynthesis of two Vietnamese species of *Sargassum*, *Sargassum mcclurei* and *Sargassum oligocystum*, based on the field and laboratory measurements. Phycol Res 64: 230–240

Terada R, Yuge T, Watanabe Y, Mine T, Morikawa T, Nishihara GN (2020b) Chronic effects of three different stressors, irradiance, temperature, and desiccation on the PSII photochemical efficiency in the heteromorphic life-history stages of cultivated *Pyropia yezoensis* f. *narawaensis* (Bangiales) from Japan. J Appl Phycol 32: 3273–3284

Thornley JHM, Johnson IR (2000) Plant and Crop Modelling: A mathematical approach to plant and crop physiology. Blackburn Press, Caldwell, NJ

Titlyanov EA, Titlyanova TV (2012) Marine plants of the Asian Pacific region countries, their use and cultivation. A.V. Zhirmunsky Institute of Marine Biology Ear East Branch of the Russian Academy of Sciences, Dalnauka, Vladivostok

Tseng CK, Lu B (2000) Flora algarum marinarum Sinicarum. Tomus III Phaeophyta, No. II Fucales. Science Press, Beijing (in Chinese)

Uchida T, Yoshikawa K, Arai A, Arai S (1991) Life-cycle and its control of *Sargassum*

muticum (Phaeophyta) in batch cultures. Nippon Suisan Gakkaishi 57: 2249–2253

Wainwright BJ, Bauman AG, Zahn GL, Todd P, Huang D (2019) Characterization of fungal biodiversity and communities associated with the reef macroalga *Sargassum ilicifolium* reveals fungal community differentiation according to geographic locality and algal structure. Mar Biodivers 49: 2601–2608

Wang WJ, Wang FJ, Zhu JY, Sun XT, Yao CY, Xu P (2011) Freezing tolerance of *Porphyra yezoensis* (Bangiales, Rhodophyta) gametophyte assessed by chlorophyll fluorescence. J Appl Phycol 23: 1017–1022

Watanabe Y, Nishihara GN, Tokunaga S, Terada R (2014) The effect of irradiance and temperature responses and the phenology of a native alga, *Undaria pinnatifida* (Laminariales), at the southern limit of its natural distribution in Japan. J Appl Phycol 26: 2405–2415

Watanabe Y, Yamada H, Mine Y, Kawamura Y, Nishihara GN, Terada R (2017) Chronological change and the potential of recovery on the photosynthetic efficiency of *Pyropia yezoensis* f. *narawaensis* (Bangiales) during the sporelings frozen storage treatment in the Japanese Nori cultivation. Phycol Res 65: 265–271

Webb WL, Newton M, Starr D (1974) Carbon dioxide exchange of *Alnus rubra*: a mathematical model. Oecologia 17: 281–291

Wernberg T, Thomsena MS, Stæhr PA, Pedersena MF (2000) Comparative Phenology of *Sargassum muticum* and *Halidrys siliquosa* (Phaeophyceae: Fucales) in Limfjorden, Denmark. Bot Mar 43: 31–39

Williams SL, Smith J (2007) A global review of the distribution, taxonomy, and impacts of introduced seaweeds. Annu Rev Ecol Evol Syst 38: 327–359

Wiltens J, Schreiber U, Vidaver W (1978) Chlorophyll fluorescence induction: an indicator of photosynthetic activity in marine algae understanding desiccation. Can J Bot 56: 2787–2794

Xie XJ, Wang XL, Lin LD, *et al.* (2016) Effects of hypo- and hypersalinity on photosynthetic performance of *Sargassum fusiforme* (Fucales, Heterokontophyta). Photosynthetica 54: 210–218

Xu GP, Terada R, Watanabe Y, Nishihara GN (2021) The occurrence of *Phycocalidia tanegashimensis* (Bangiaceae) in the splash zone may be related to the tolerance of photochemical efficiency to temperature, irradiance, desiccation, and salinity. J Appl Phycol 33: 3427–3435

Xu Z, Gao G, Xu J, Wu H (2017) Physiological response of a golden tide alga (*Sargassum muticum*) to the interaction of ocean acidification and phosphorus enrichment. Biogeosciences 14: 671–681

Yatsuya K, Nishigaki T, douke A, Wada T (2005) Annual net production of the five Sargassaceae species in Yoro, western Wakasa Bay, Sea of Japan. Fish Sci 71: 1098–1106

Yendo K (1907) The Fucaceae of Japan. J Coll Sci Imp Univ Tokyo 21: 1–174

Yonemori Y, Kokubu S, Nishihara GN, Endo H, Terada R (2023) The effects of desiccation and salinity gradients in the *PSII* photochemical efficiency of an intertidal brown alga, *Sargassum fusiforme* from Kagoshima, Japan. Phycol. Res. 71: DOI: 10.1111/PRE.12491 (online).

Yoshida G, Shimabukuro H (2017) Seasonal population dynamics of *Sargassum fusiforme* (Fucales, Phaeophyta), Suo-Oshima Is., Seto Inland Sea, Japan–development processes of a stand characterized by high density and productivity. J Appl Phycol 29: 639–648

Yoshida T (1983) Japanese species of *Sargassum* subgenus *Bactrophycus* (Phaeophyta, Fucales). J Fac Sci Hokkaido Univ Ser 5 Bot 13: 99–246

Yoshida T (1998) Marine algae of Japan. Uchida Rokakuho, Tokyo (in Japanese)

Figure Legends

Fig. 1. The response of the net photosynthetic rates of *Sargassum muticum* from the native range of distribution at Yura, Awaji-shima Island, Hyogo, Japan to irradiance at (a) 8°C, (b) 20°C, and (c) 28°C. The dots indicate the actual measured rates (n = 5 per level), the lines indicate the expected value, and the shaded regions indicate the 95% Bayesian prediction interval (BPI) of the model.

Fig. 2. The response of the oxygenic photosynthesis and dark respiration of *Sargassum muticum* from the native range of distribution at Yura, Awaji-shima Island, Hyogo, Japan to temperature (8–36°C, every four increment). Net photosynthesis measurements were done at 300 µmol photons m^{-2} s^{-1}, and the dark respirations at 0 µmol photons m^{-2} s^{-1} (n = 5 per temperature). (a) The net photosynthesis to temperature determined at 300 µmol photons m^{-2} s^{-1}. (b) The modeled gross photosynthetic rates at 300 µmol photons m^{-2} s^{-1}. Data were derived from the model curve of net photosynthesis (a) and dark respiration (c). The dark respiration rate to temperature at 0 µmol photons m^{-2} s^{-1}. See the caption in Fig.1 for the details. Note that the shaded region for (b) is the 95% BPI of the expected value.

Fig. 3. The response of photochemical efficiency (F_v/F_m) in *Sargassum muticum* from the native range of distribution at Yura, Awaji-shima Island, Hyogo, Japan at nine temperature treatments (8, 12, 16, 20, 24, 28, 30, 32, and 36°C) after (a) 24, (b) 48, and (c) 72 hours without light. The dots indicate the actual measured values (n = 10 per temperature), the lines indicate the expected value, and the shaded regions indicate the 95% Bayesian prediction interval (BPI) of the expectation.

Fig. 4. The hourly response of photochemical efficiency ($\Delta F/F_m'$) in *Sargassum muticum* from the native range of distribution at Yura, Awaji-shima Island, Hyogo, Japan to irradiance at 200 µmol photons m^{-2} s^{-1} (circle) and 1000 µmol photons m^{-2} s^{-1} (triangle), under (a, b) 8°C, (c, d) 20°C, and (e, f) 28°C. The symbols indicate the average of measured values (n = 10), and bars indicate standard deviation. Initial values and the values after 12-hour dark acclimation were measured as F_v/F_m.

Fig. 5. The chronological change of photochemical efficiency ($\Delta F/F_m'$) in *Sargassum muticum* from the native range of distribution at Yura, Awaji-shima Island, Hyogo, Japan during desiccation and rehydration at 50% humidity under (a) dim-light (20 µmol photons m^{-2} s^{-1}) and (b) high irradiance (700 µmol photons m^{-2} s^{-1}, triangle). Desiccation

experiments were carried out for 0.5, 1, 2, 3, 4, 6, and 8 h. The closed circle, triangle, and rectangle dots indicate measurements exposed in air, those in subsequent 30-minute and 24-hour rehydration in seawater at each desiccation period treatments. The symbols indicate the average of actual values measured (n = 50), and bars indicate standard deviation.

Fig. 6. The relationship between photochemical efficiency ($\Delta F/F_m'$) and the absolute water content (AWC, %) in *Sargassum muticum* from the native range of distribution at Yura, Awaji-shima Island, Hyogo, Japan to aerial exposure at the 50% humidity under the (a, c, e) dim light (20 µmol photons m^{-2} s^{-1}) and (b, d, f) high irradiance (700 µmol photons m^{-2} s^{-1}). The symbols indicate the average of actual values measured (n = 10), and bars indicate standard deviation. (a, b), (c, d), and (e, f) indicate measurements exposed in air, those in subsequent 30-min and 24-hour rehydration in seawater, respectively.

Fig. 7. The response of the net photosynthetic rates of *Sargassum macrocarpum* from Yamaguchi, Japan to irradiance under white (A) light (metal halide lamp), red (B), green (C), and blue (D) light-emitting diode (LED) arrays at 24°C. The dots indicate the mean measured rates (n = 5 with standard deviation), the lines indicate the expected value, and

the shaded regions indicate the 95% highest density credible interval (95% HDCI) of the predictions.

Fig. 8. The response of photochemical efficiency (F_v/F_m and $\Delta F/F_m'$) of the photosystem II in *Sargassum macrocarpum* from Yamaguchi, Japan to temperature (4, 8, 12, 16, 20, 24, 28, 30, 32, and 36°C) under 0 (A, B, C; as F_v/F_m) and 50 (D, E, F; as $\Delta F/F_m'$) µmol photons m^{-2} s^{-1} (12L:12D photoperiod) after 1- (A, D), 3- (B, E), and 6-day culture (C, F). The dots indicate the mean measured values (n = 10 with standard deviation), the lines indicate the expected value, and the shaded regions indicate the 95% highest density credible intervals (95% HDCI) of the model.

Fig. 9. The chronological change of photochemical efficiency ($\Delta F/F_m'$) of the photosystem II in *Sargassum macrocarpum* from Yamaguchi, Japan during desiccation and rehydration at 24°C and 50% humidity under 20 µmol photons m^{-2} s^{-1}. Desiccation experiments were carried out at 0 (not desiccated), 0.1 (10-min), 0.5 (30-min), 0.75 (45-min), 1, 1.5, 2, 4, and 8 hours. The symbols indicate measurements exposed in air (purple dots), and in subsequent 30-minute (blue dots) and 1-day rehydration (green dots) in seawater at each desiccation treatment. The symbols indicate the mean measured values

(n = 50 with standard deviation), and bars indicate standard errors.

Fig. 10. The relationship between photochemical efficiency ($\Delta F/F_m'$) of photosystem II and the absolute water content (AWC, %) in *Sargassum macrocarpum* from Yamaguchi, Japan to aerial exposure at 24°C and 50% humidity under 20 µmol photons m^{-2} s^{-1}. The graphs indicate measurements exposed in air (A), and in subsequent 30-minute (B) and 1-day rehydration (C) in seawater at each desiccation treatment. These dots indicate each mean measured values (n = 10), the lines indicate the fitted model, and the shaded regions is the 95% highest density credible intervals (HDCI) of the model.

Fig. 11. The response of photochemical efficiency ($\Delta F/F_m'$) of photosystem II in *Sargassum macrocarpum* from Yamaguchi, Japan at eleven salinity treatments (0, 5, 10, 20, 30, 34, 40, 50, 60, 70, and 80 psu) after 1 (A), 2 (B), and 3 (C) day culture under 24°C and 20 µmol photons m^{-2} s^{-1} (photoperiod of 12L:12D). The symbols indicate the mean measured values (n = 10 with standard deviation), the lines indicate the fitted model, and the shaded regions is the 95% highest density credible intervals (HDCI) of the model.

Table 1. Mean and 95% Bayesian highest density credible intervals (95% HDCI) of net photosynthesis – irradiance (*P*–*E*) parameters of *Sargassum muticum* from the native range of distribution at Yura, Awaji-shima Island, Hyogo, Japan at 8, 20, and 28 °C. NP_{max} = maximum net photosynthesis (μg O_2 g_{ww}^{-1} min^{-1}); α = initial slope [μg O_2 g_{ww}^{-1} min^{-1} (μmol photons m^{-2} s^{-1}) $^{-1}$]; R_d = respiration rate (μg O_2 g_{ww}^{-1} min^{-1}); E_c = compensation irradiance (μmol photons m^{-2} s^{-1}); E_k = saturation irradiance (μmol photons m^{-2} s^{-1}).

	8 °C		**20 °C**		**28 °C**	
Parameter	**Mean**	**95% HDCI**	**Mean**	**95% HDCI**	**Mean**	**95% HDCI**
NP_{max}	5.16	4.96 – 5.36	11.88	11.37 – 12.39	28.12	21.62 – 34.62
α	0.05	0.05 – 0.05	0.06	0.06 – 0.06	0.04	0.03 – 0.05
R_d	0.23	0.14 – 0.32	0.20	0.11 – 0.29	0.15	0.07 – 0.23
E_c	5	2 – 7	3	2 – 5	4	2 – 5
E_k	110	98 – 121	200	180 – 220	753	473 – 1034

Table 2. Mean and 95% highest density credible intervals (HDCI**)** of parameters estimated for gross photosynthesis – temperature (*P*–*T*) model of *Sargassum muticum* from the native range of distribution at Yura, Awaji-shima Island, Hyogo, Japan. GP_{max} = maximum gross photosynthesis (μg O_2 g_{ww}^{-1} min^{-1}); H_a = activation energy for photosynthesis (kJ mol^{-1}); H_d = deactivation energy (kJ mol^{-1}); T_{opt}^{GP} = optimum temperature (°C); E_a = activation energy for respiration (kJ mol^{-1}); R_{22} = respiration rate at 22°C (μg O_2 g_{ww}^{-1} min^{-1}).

Parameter	**Mean**	**95% HDCI**
$\boldsymbol{GP_{max}}$	9.57	9.06 – 10.08
$\boldsymbol{H_a}$	36.5	16.3 – 56.7
$\boldsymbol{H_d}$	116.7	90.2 – 143.3
$\boldsymbol{T_{opt}^{GP}}$	19.5	17.2 – 21.9
$\boldsymbol{E_a}$	0.29	0.26 – 0.32
$\boldsymbol{R_{22}}$	9.57	9.06 – 10.08

Table 3. Mean and 95% highest density credible intervals (HDCI) of the parameters estimated for the maximum quantum yield in photosystem II (F_v/F_m) – temperature model in *Sargassum muticum* from the native range of distribution at Yura, Awaji-shima Island, Hyogo, Japan exposed for 24, 48, and 72 h. $F_v/F_{m\ (max)}$ = maximum quantum yield; H_a = activation energy for photosynthesis (kJ mol^{-1}); H_d = deactivation energy (kJ mol^{-1}); $T_{opt}^{Fv/Fm}$ = optimum temperature (°C), π = probability of zero.

	24 h		48 h		72 h	
Parameter	**Mean**	**95% HDCI**	**Mean**	**95% HDCI**	**Mean**	**95% HDCI**
$F_v/F_{m\ (max)}$	0.68	0.67 – 0.68	0.68	0.67 – 0.69	0.67	0.66 – 0.69
$\boldsymbol{H_a}$	2	1 – 3	2	1 – 2	2	1 – 3
$\boldsymbol{H_d}$	197	128 – 270	244	173 – 312	497	401 – 594
$\boldsymbol{T_{opt}^{Fv/Fm}}$	19.9	17.2 – 22.5	19.6	17.0 – 22.1	23.5	22.1 – 24.8
$\boldsymbol{\pi}$	0.80	0.41 – 1.26	0.80	0.39 – 1.23	0.81	0.38 – 1.24

Table 4. Mean and 95% highest density credible intervals (95% HDCI) of net photosynthesis – irradiance (*P*–*E*) parameters of *Sargassum*

macrocarpum from Yamaguchi, Japan under different light spectra (white, red, green and blue light) at 24°C. NP_{max} = maximum net photosynthesis (µg O_2 g_{ww}^{-1} min^{-1}); α = initial slope [µg O_2 g_{ww}^{-1} min^{-1} (µmol photons m^{-2} s^{-1}) $^{-1}$]; R_d = respiration rate (µg O_2 g_{ww}^{-1} min^{-1}); E_c = compensation irradiance (µmol photons m^{-2} s^{-1}); E_k = saturation irradiance (µmol photons m^{-2} s^{-1}).

	White light		Red light		Green light		Blue light	
Parameter	**Mean**	**95% HDCI**	**Mean**	**95% HDCI**	**Mean**	**95% HDCI**	**Mean**	**95% HDCI**
NP_{max}	24.4	22.6 – 26.0	8.18	6.68 – 9.73	12.3	10.6 – 14.0	22.1	19.7 – 24.9
α	0.11	0.09 – 0.13	0.11	0.06 – 0.17	0.06	0.04 – 0.09	0.06	0.05 – 0.07
R_d	2.89	1.78 – 4.02	1.81	0.53 – 3.18	1.37	0.28 – 2.55	2.79	1.76 – 3.82
E_c	27.7	18.9 – 35.9	19.0	7.37 – 30.1	23.5	5.99 – 38.0	52.2	37.4 – 65.4
E_k	221	187 – 261	80.2	48.7 – 123	209	140 – 308	394	305 – 514

Table 5. The mean and 95% highest density credible intervals (95% HDCI) of the parameters estimated for the maximum quantum yield (F_v/F_m) – temperature model in *Sargassum macrocarpum* from Yamaguchi, Japan exposed for 1-, 3-, and 6-day culture. F_v/F_m = maximum quantum yield; H_a = activation energy for photosynthesis (kJ mol^{-1}); H_d = deactivation energy (kJ mol^{-1}); $T_{opt}^{Fv/Fm}$ = optimum temperature (°C).

	1-d		3-d		6-d	
Parameter	**Mean**	**95% HDCI**	**Mean**	**95% HDCI**	**Mean**	**95% HDCI**
$\boldsymbol{F_v/F_{m\,(max)}}$	0.651	0.626 – 0.678	0.632	0.609 – 0.656	0.603	0.588 – 0.619
$\boldsymbol{H_a}$	5.11	3.15 – 7.74	4.72	2.47 – 9.02	11.7	0.872 – 56.6
$\boldsymbol{H_d}$	289	173 – 418	212	84.7 –376	64.8	14.2 – 167
$\boldsymbol{T_{opt}^{Fv/Fm}}$	21.8	18.3 – 24.3	18.9	13.6 – 22.7	20.1	14.9 – 27.0

Table 6. The mean and 95% highest density credible intervals (95% HDCI) of the parameters estimated for the effective quantum yield ($\Delta F/F_m'$) – temperature model in *Sargassum macrocarpum* from Yamaguchi, Japan exposed for 1-, 3-, and 6-day culture. $\Delta F/F_m'$ = effective quantum yield; H_a = activation energy for photosynthesis (kJ mol^{-1}); H_d = deactivation energy (kJ mol^{-1}); $T_{opt}^{\Phi F/Fm'}$ = optimum temperature (°C).

	1-d		3-d		6-d	
Parameter	**Mean**	**95% HDCI**	**Mean**	**95% HDCI**	**Mean**	**95% HDCI**
$\boldsymbol{\Delta F/F_m'_{(max)}}$	0.545	0.526 – 0.567	0.634	0.600 – 0.669	0.582	0.556 – 0.611
$\boldsymbol{H_a}$	121	91.1 – 153	24.7	19.2 – 30.9	126	84.0 – 168
$\boldsymbol{H_d}$	139	116 – 165	376	287 – 480	141	112 –176
$\boldsymbol{T_{opt}^{\Delta F/Fm'}}$	20.5	19.2 – 21.9	26.4	25.1 – 27.7	22.4	20.3 – 25.3

Table 7. Mean values of the effective quantum yield ($\Delta F/F_m'$) in *Sargassum macrocarpum* from Yamaguchi, Japan at eleven salinity treatments (0, 5, 10, 20, 30, 34, 40, 50, 60, 70, and 80 psu) after 1-, 2-, and 3-day culture under 24°C and 20 µmol photons m^{-2} s^{-1} (photoperiod of 12L:12D; n = 10, standard deviation, SD).

Salinity	1-day	2-day	3-day
80	0.000 ± 0.000	0.000 ± 0.000	0.000 ± 0.000
70	0.000 ± 0.000	0.000 ± 0.000	0.000 ± 0.000
60	0.000 ± 0.000	0.000 ± 0.000	0.000 ± 0.000
50	0.125 ± 0.178	0.055 ± 0.127	0.000 ± 0.000
40	0.610 ± 0.022	0.597 ± 0.018	0.595 ± 0.014
34	0.609 ± 0.016	0.608 ± 0.004	0.602 ± 0.014
30	0.592 ± 0.012	0.613 ± 0.008	0.601 ± 0.006
20	0.549 ± 0.049	0.579 ± 0.027	0.554 ± 0.045
10	0.341 ± 0.222	0.109 ± 0.198	0.037 ± 0.111
5	0.096 ± 0.067	0.000 ± 0.000	0.000 ± 0.000
0	0.000 ± 0.000	0.000 ± 0.000	0.000 ± 0.000

Fig.1

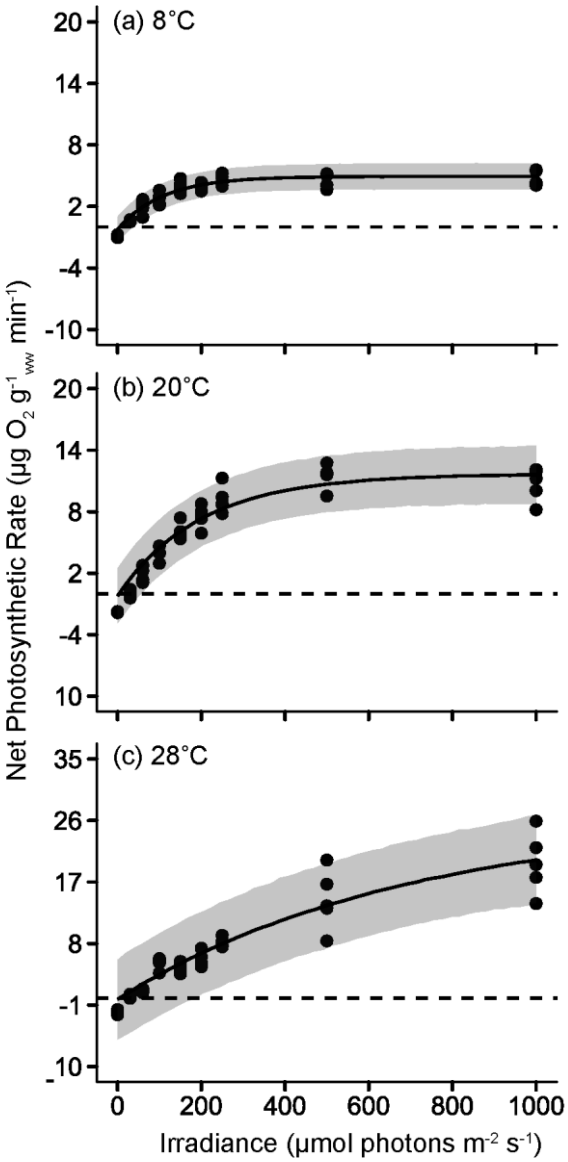

Fig. 1. The response of the net photosynthetic rates of *Sargassum muticum* from the native range of distribution at Yura, Awaji-shima Island, Hyogo, Japan to irradiance at (a) 8°C, (b) 20°C, and (c) 28°C. The dots indicate the actual measured rates (n = 5 per level), the lines indicate the expected value, and the shaded regions indicate the 95% Bayesian prediction interval (BPI) of the model.

Fig.2

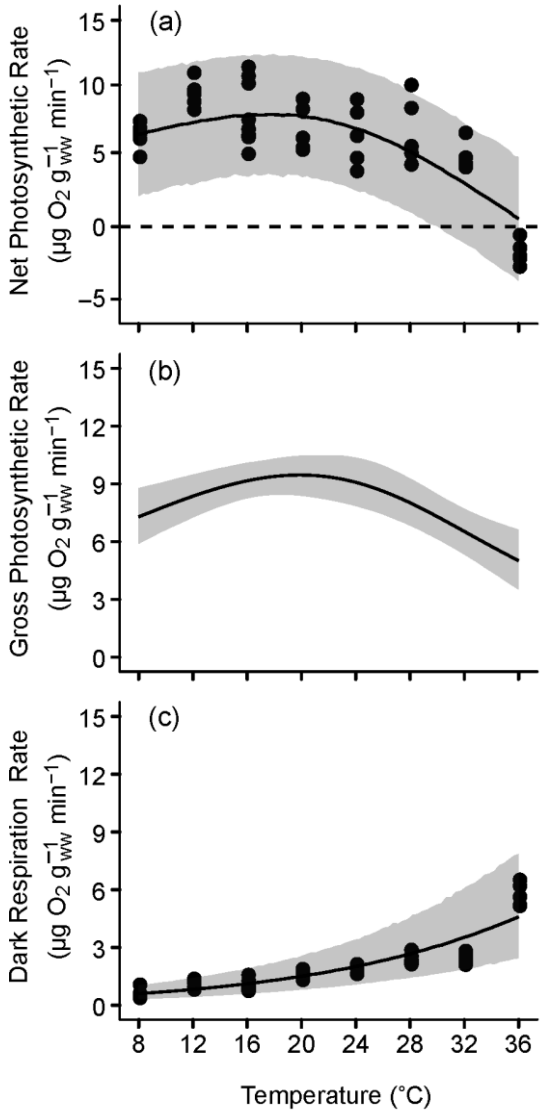

Fig. 2. The response of the oxygenic photosynthesis and dark respiration of *Sargassum muticum* from the native range of distribution at Yura, Awaji-shima Island, Hyogo, Japan to temperature (8–36°C, every four increment). Net photosynthesis measurements were done at 300 μmol photons m^{-2} s^{-1}, and the dark respirations at 0 μmol photons m^{-2} s^{-1} (*n* = 5 per temperature). (a) The net photosynthesis to temperature determined at 300 μmol photons m^{-2} s^{-1}. (b) The modeled gross photosynthetic rates at 300 μmol photons m^{-2} s^{-1}. Data were derived from the model curve of net photosynthesis (a) and dark respiration (c). The dark respiration rate to temperature at 0 μmol photons m^{-2} s^{-1}. See the caption in Fig.1 for the details. Note that the shaded region for (b) is the 95% BPI of the expected value.

Fig. 3.

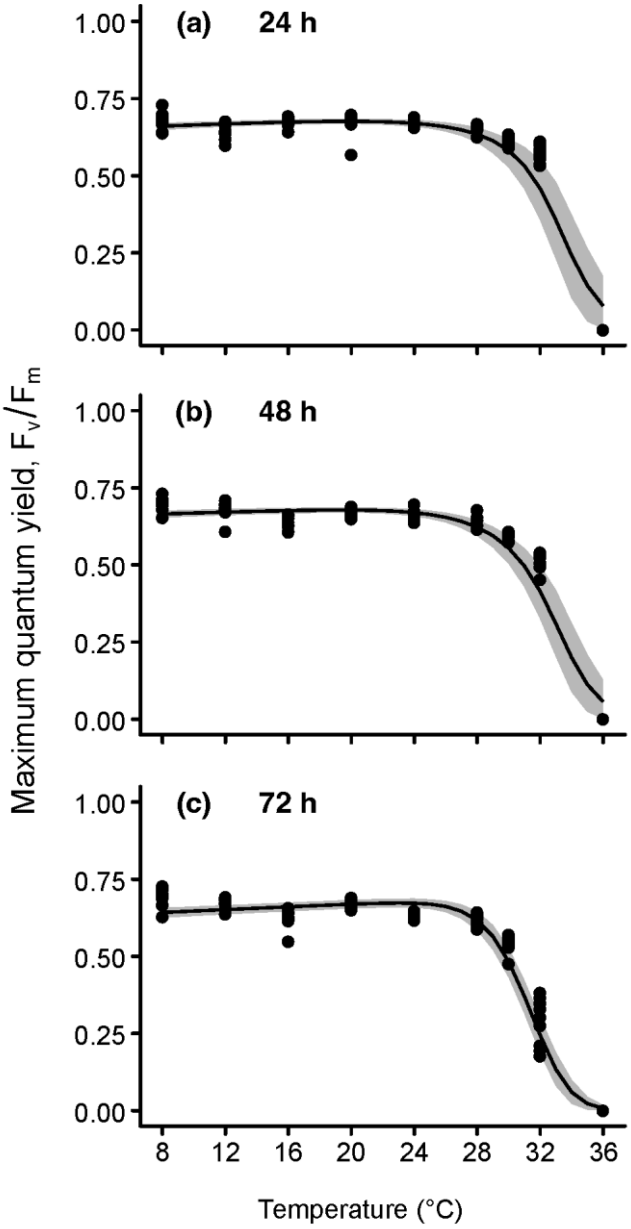

Fig. 3. The response of photochemical efficiency (F_v/F_m) in *Sargassum muticum* from the native range of distribution at Yura, Awaji-shima Island, Hyogo, Japan at nine temperature treatments (8, 12, 16, 20, 24, 28, 30, 32 and 36°C) after (a) 24, (b) 48, and (c) 72 hours without light. The dots indicate the actual measured values (n = 10 per temperature), the lines indicate the expected value, and the shaded regions indicate the 95% Bayesian prediction interval (BPI) of the expectation.

Fig.4

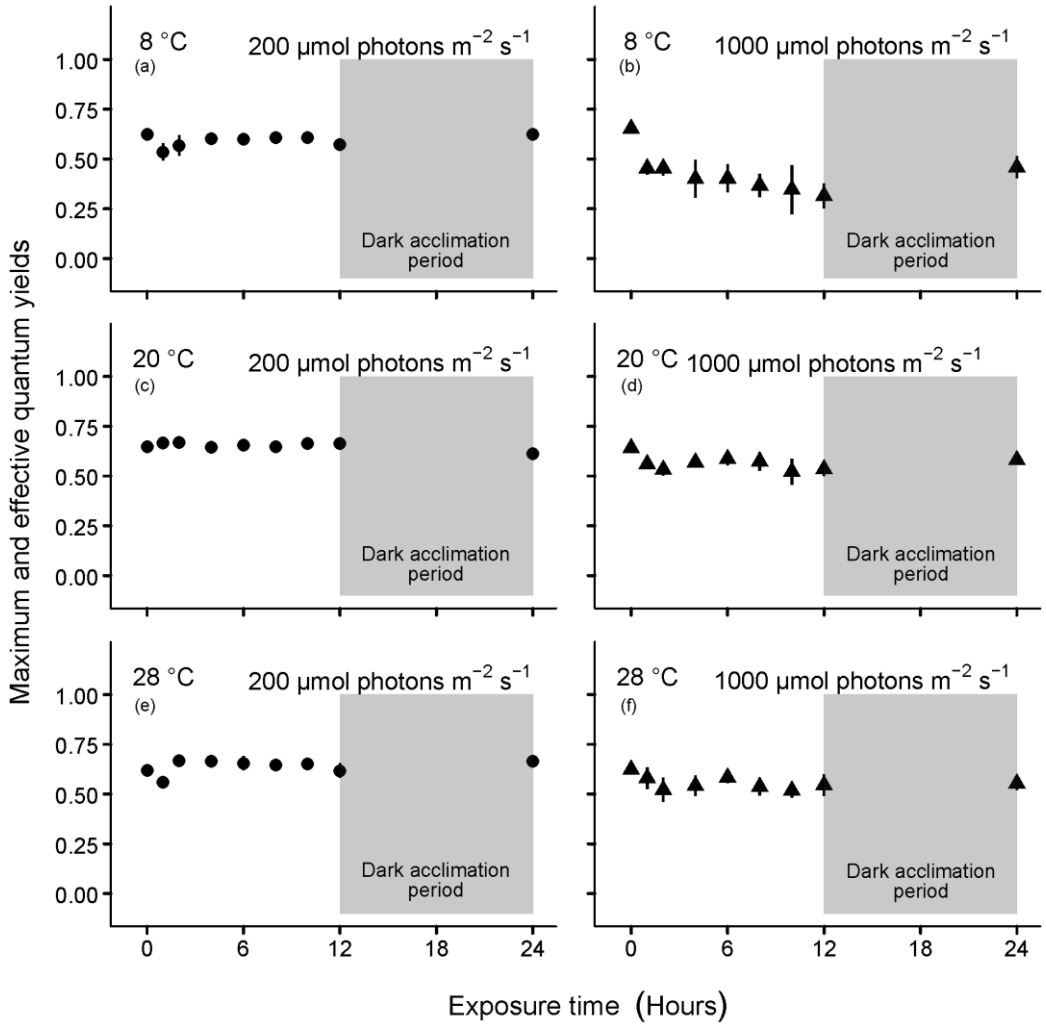

Fig. 4. The hourly response of photochemical efficiency ($\Delta F/F_m'$) in *Sargassum muticum* from the native range of distribution at Yura, Awaji-shima Island, Hyogo, Japan to irradiance at 200 µmol photons m^{-2} s^{-1} (circle) and 1000 µmol photons m^{-2} s^{-1} (triangle), under (a, b) 8°C, (c, d) 20°C, and (e, f) 28°C. The symbols indicate the average of measured values (n = 10), and bars indicate standard deviation. Initial values and the values after 12-hour dark acclimation were measured as F_v/F_m.

Fig. 5

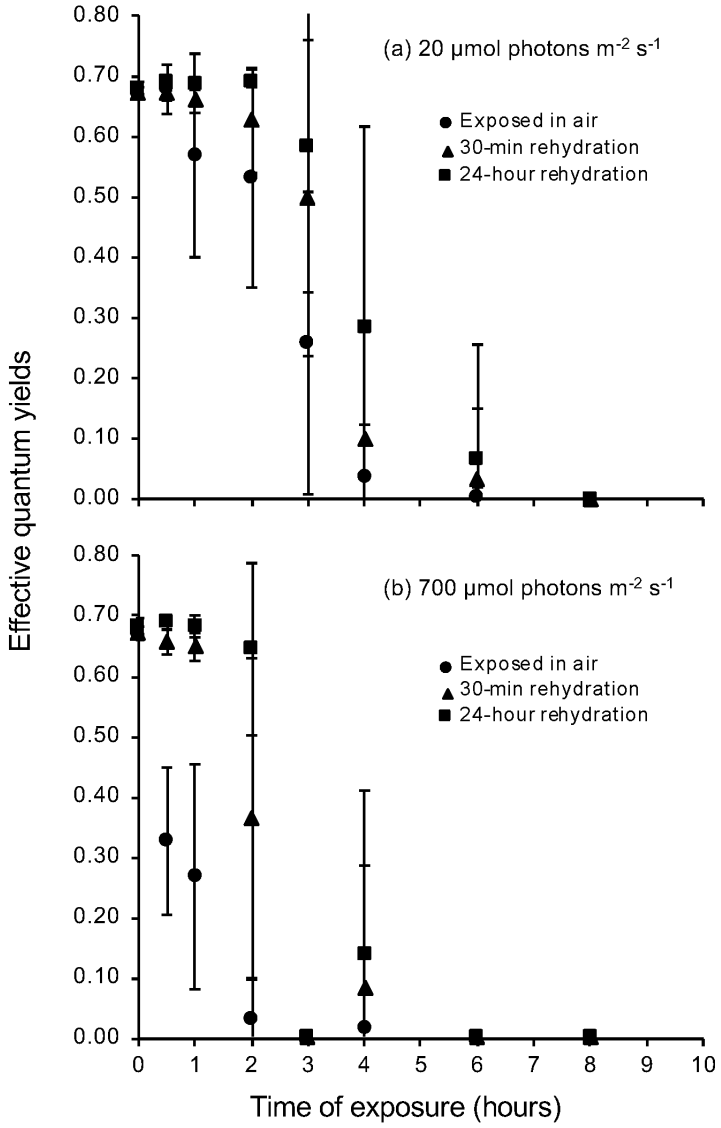

Fig. 5. The chronological change of photochemical efficiency ($\Delta F/F_m'$) in *Sargassum muticum* from the native range of distribution at Yura, Awaji-shima Island, Hyogo, Japan during desiccation and rehydration at 50% humidity under (a) dim-light (20 µmol photons m^{-2} s^{-1}) and (b) high irradiance (700 µmol photons m^{-2} s^{-1}, triangle). Desiccation experiments were carried out for 0.5, 1, 2, 3, 4, 6, and 8 h. The closed circle, triangle, and rectangle dots indicate measurements exposed in air, those in subsequent 30-minute and 24-hour rehydration in seawater at each desiccation period treatments. The symbols indicate the average of actual values measured (n = 50), and bars indicate standard deviation.

Fig. 6

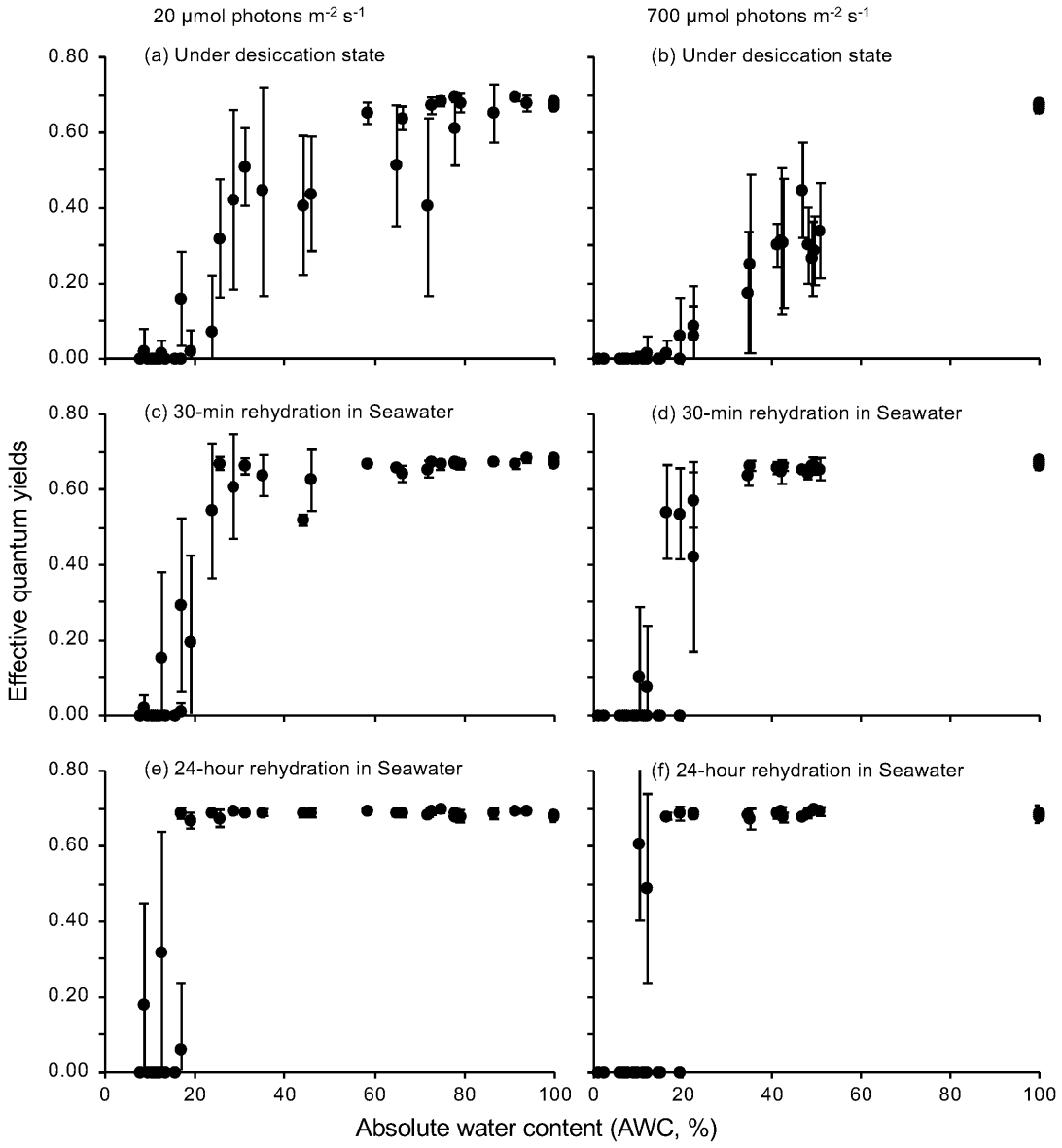

Fig. 6. The relationship between photochemical efficiency ($\Delta F/F_m'$) and the absolute water content (AWC, %) in *Sargassum muticum* from the native range of distribution at Yura, Awaji-shima Island, Hyogo, Japan to aerial exposure at the 50% humidity under the (a, c, e) dim light (20 µmol photons m^{-2} s^{-1}) and (b, d, f) high irradiance (700 µmol photons m^{-2} s^{-1}). The symbols indicate the average of actual values measured (n = 10), and bars indicate standard deviation. (a, b), (c, d), and (e, f) indicate measurements exposed in air, those in subsequent 30-min and 24-hour rehydration in seawater, respectively.

Fig. 7

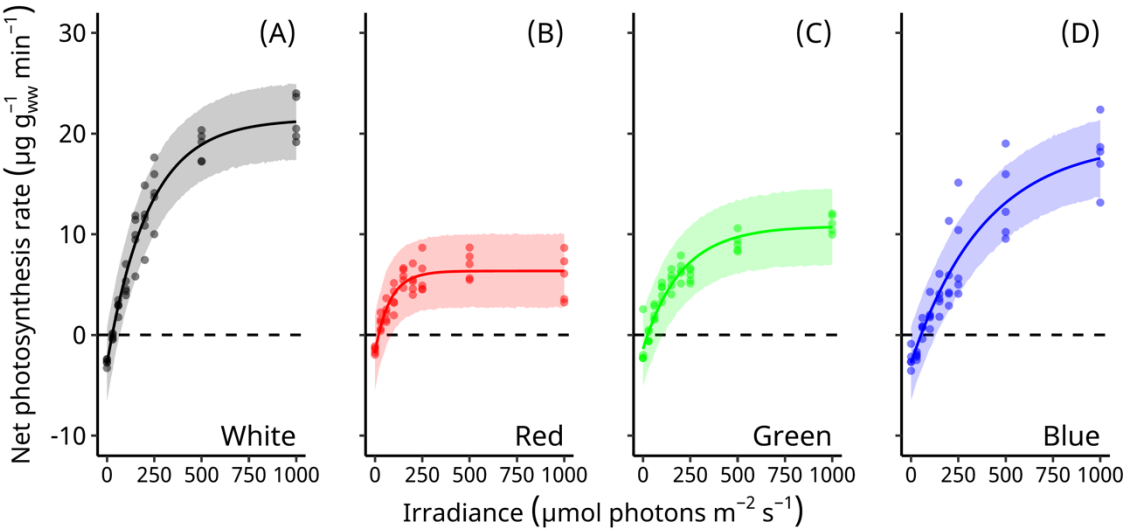

Fig. 7. The response of the net photosynthetic rates of *Sargassum macrocarpum* from Yamaguchi, Japan to irradiance under white (A) light (metal halide lamp), red (B), green (C), and blue (D) light-emitting diode (LED) arrays at 24°C. The dots indicate the mean measured rates (n = 5 with standard deviation), the lines indicate the expected value, and the shaded regions indicate the 95% highest density credible interval (95% HDCI) of the predictions.

Fig. 8

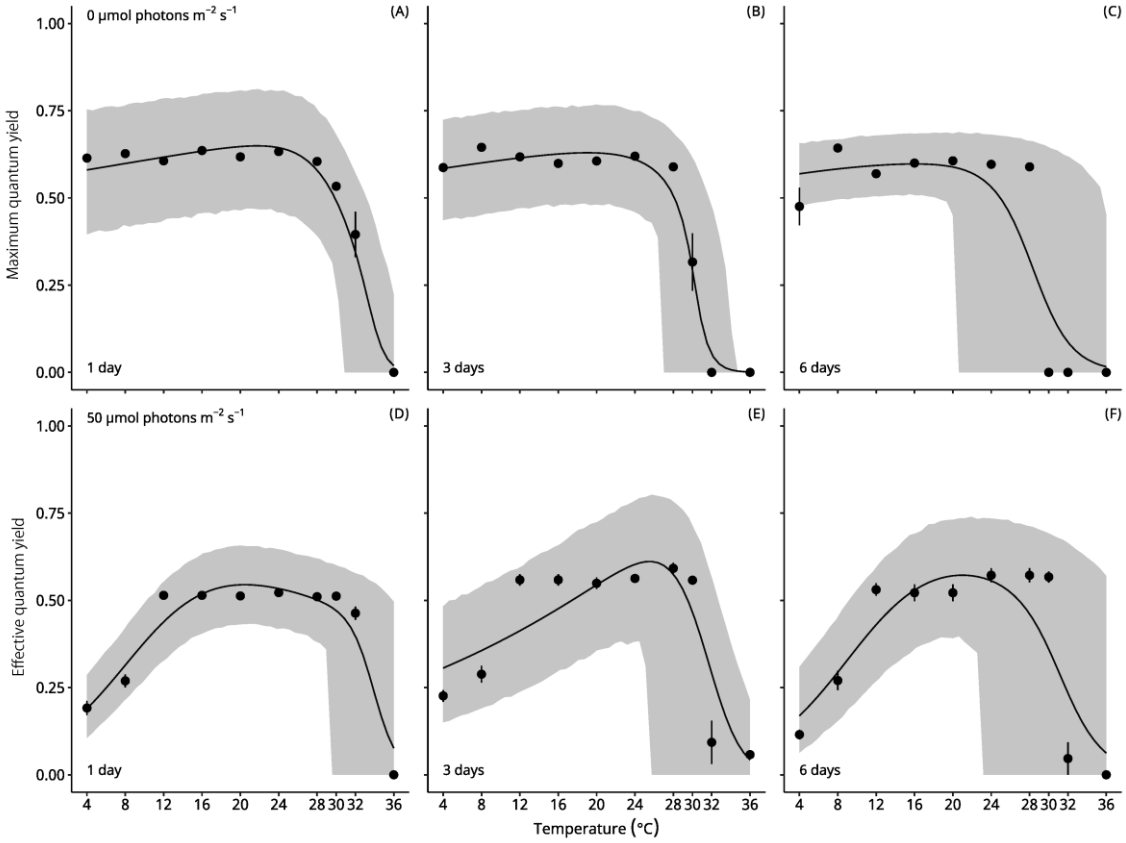

Fig. 8. The response of photochemical efficiency (F_v/F_m and $\Delta F/F_m'$) of the photosystem II in *Sargassum macrocarpum* from Yamaguchi, Japan to temperature (4, 8, 12, 16, 20, 24, 28, 30, 32, and 36°C) under 0 (A, B, C; as F_v/F_m) and 50 (D, E, F; as $\Delta F/F_m'$) µmol photons m^{-2} s^{-1} (12L:12D photoperiod) after 1- (A, D), 3- (B, E), and 6-day culture (C, F). The dots indicate the mean measured values (n = 10 with standard deviation), the lines indicate the expected value, and the shaded regions indicate the 95% highest density credible intervals (95% HDCI) of the model.

Fig. 9

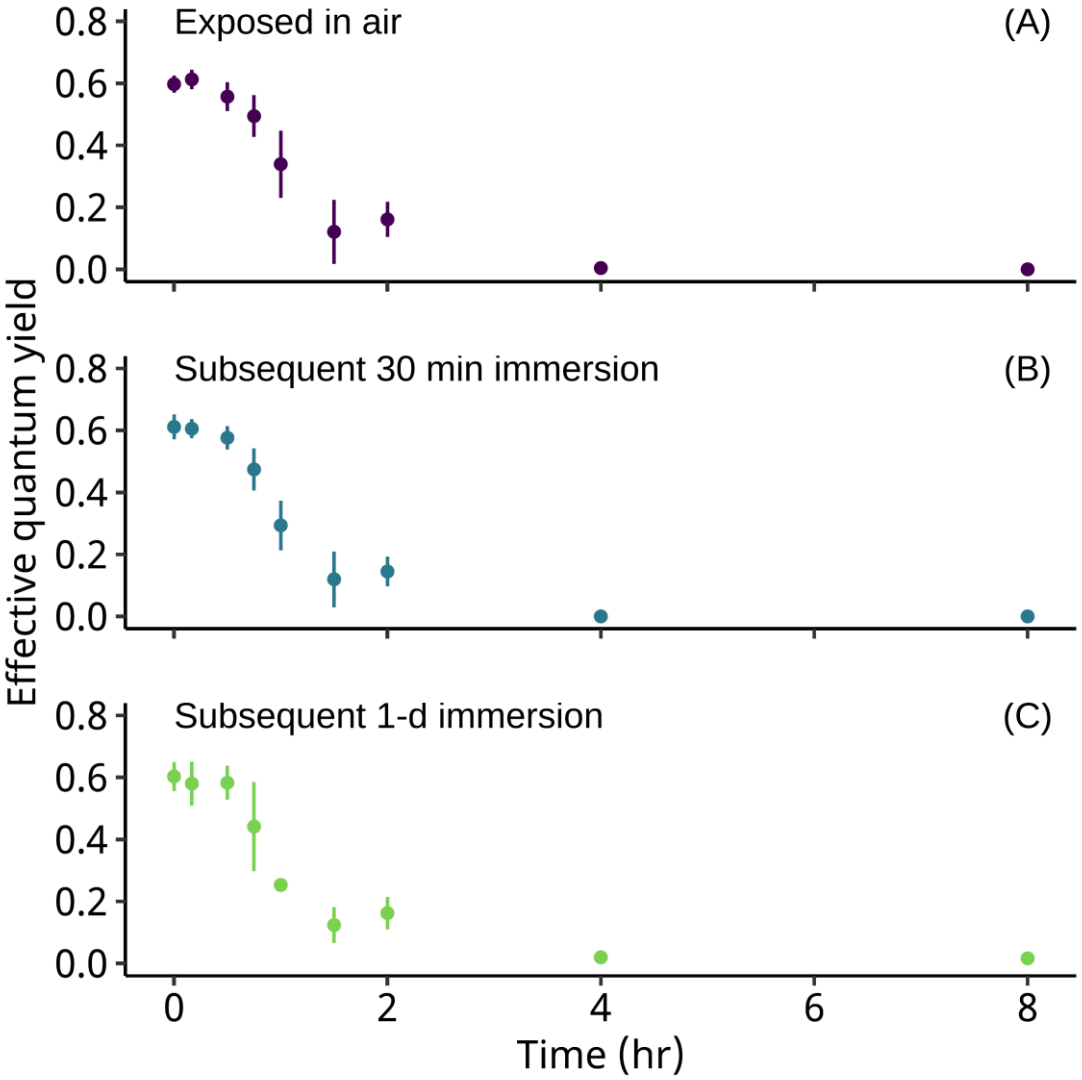

Fig. 9. The chronological change of photochemical efficiency ($\Delta F/F_m'$) of the photosystem II in *Sargassum macrocarpum* from Yamaguchi, Japan during desiccation and rehydration at 24°C and 50% humidity under 20 µmol photons m^{-2} s^{-1}. Desiccation experiments were carried out at 0 (not desiccated), 0.1 (10-min), 0.5 (30-min), 0.75 (45-min), 1, 1.5, 2, 4, and 8 hours. The symbols indicate measurements exposed in air (purple dots), and in subsequent 30-minute (blue dots) and 1-day rehydration (green dots) in seawater at each desiccation treatment. The symbols indicate the mean measured values (n = 50 with standard deviation), and bars indicate standard errors.

Fig. 10

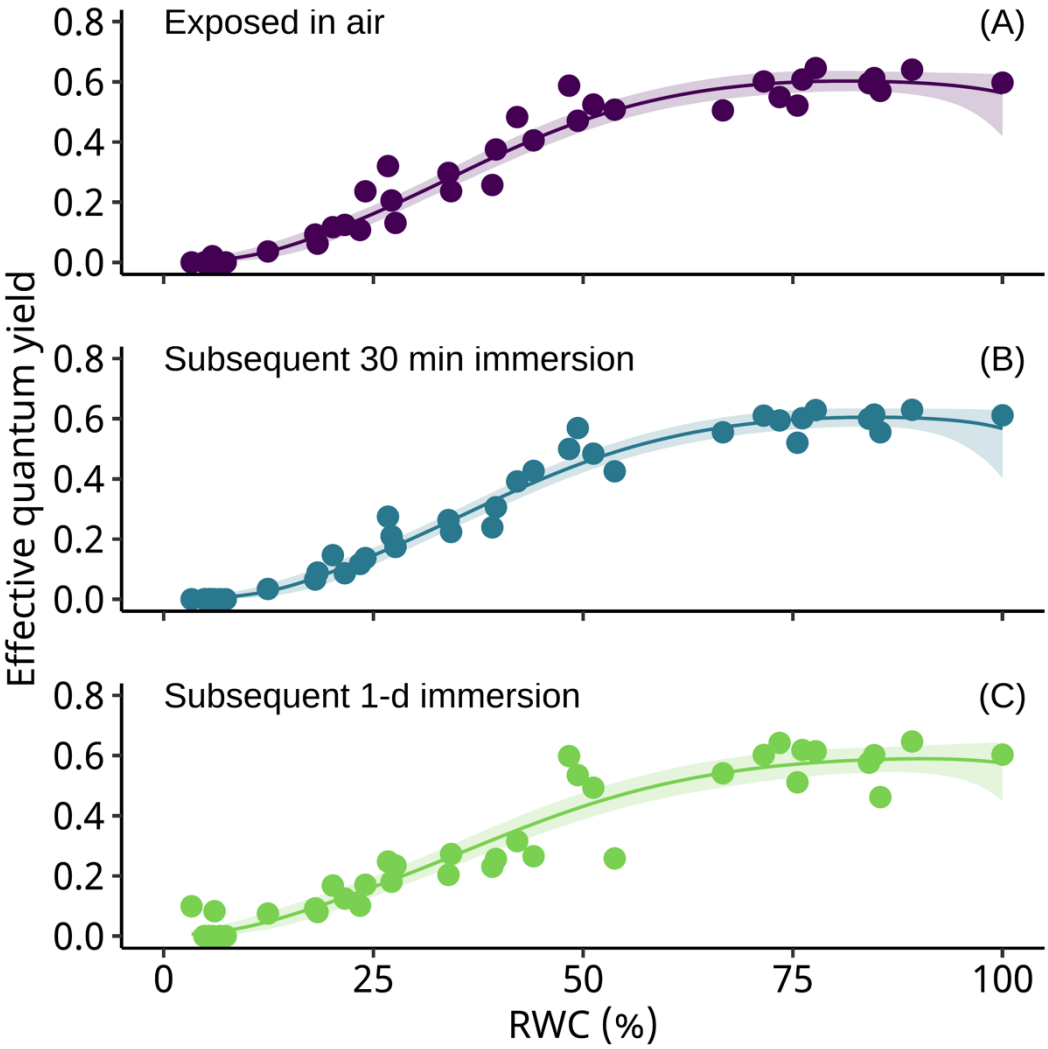

Fig. 10. The relationship between photochemical efficiency ($\Delta F/F_m'$) of photosystem II and the absolute water content (AWC, %) in *Sargassum macrocarpum* from Yamaguchi, Japan to aerial exposure at 24°C and 50% humidity under 20 µmol photons m^{-2} s^{-1}. The graphs indicate measurements exposed in air (A), and in subsequent 30-minute (B) and 1-day rehydration (C) in seawater at each desiccation treatment. These dots indicate each mean measured values (n = 10), the lines indicate the fitted model, and the shaded regions is the 95% highest density credible intervals (HDCI) of the model.

Fig. 11

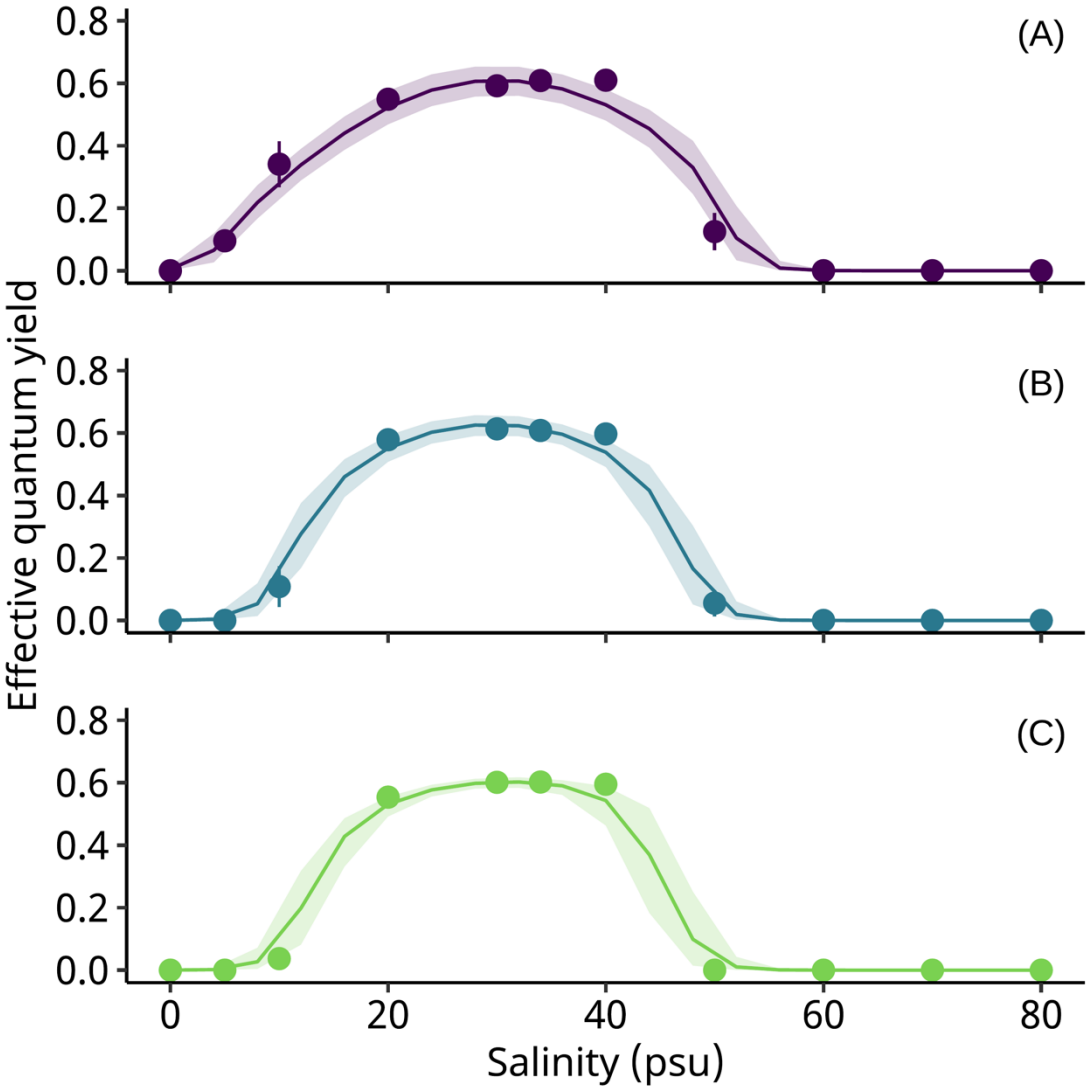

Fig. 11. The response of photochemical efficiency ($\Delta F/F_m'$) of photosystem II in *Sargassum macrocarpum* from Yamaguchi, Japan at eleven salinity treatments (0, 5, 10, 20, 30, 34, 40, 50, 60, 70, and 80 psu) after 1 (A), 2 (B), and 3 (C) day culture under 24°C and 20 µmol photons m^{-2} s^{-1} (photoperiod of 12L:12D). The symbols indicate the mean measured values (n = 10 with standard deviation), the lines indicate the fitted model, and the shaded regions is the 95% highest density credible intervals (HDCI) of the model.